ALLAN VICTOR MARTINS ALMEIDA

AN INTEGRATED MULTI-LAYERED ANALYSIS ON *DESMONOSTOC*

Dissertation presented to the Universidade Federal de Viçosa as part of requirement of the Plant Physiology Graduate Program for the obtention of the degree of *Magister Scientiae.*

VIÇOSA
MINAS GERAIS - BRAZIL
2019

Ficha catalográfica preparada pela Biblioteca Central da Universidade Federal de Viçosa - Câmpus Viçosa

T
A447i
2019

Almeida, Allan Victor Martins, 1995-
An integrated multi-layered analysis on *Desmonostoc* / Allan Victor Martins Almeida. – Viçosa, MG, 2019.
vii, 53f. : il. (algumas color.) ; 29 cm.

Texto em inglês.
Orientador: Wagner Luiz Araujo.
Dissertação (mestrado) - Universidade Federal de Viçosa.
Inclui bibliografia.

1. Cianobactéria. 2. Fisiologia. 3. Filogenia. I. Universidade Federal de Viçosa. Departamento de Biologia Vegetal. Programa de Pós-Graduação em Fisiologia Vegetal. II. Título.

CDD 22 ed. 579.39

ALLAN VICTOR MARTINS ALMEIDA

AN INTEGRATED MULTI-LAYERED ANALYSIS ON *DESMONOSTOC*

Dissertation presented to the Universidade Federal de Viçosa as part of the requirement of the Plant Physiology Graduate Program for the obtention of the degree of *Magister Scientiae*.

APPROVED: July 31, 2019.

Diego Bonaldo Genuário

Adriano Nunes Nesi

Marcelo Gomes Marçal Vieira Vaz
(Co-adviser)

Wagner Luiz Araújo
(Advisor)

ACKNOWLEDGMENTS

To my parents, Simone and Ivanilson, who always gave me support and believed in my choices.

To Wagner L. Araújo, for his advice, trust, disposition and support at all time that I needed.

To Marcelo Vaz, my co-advisor, that not only help me in this work but taught me a lot about everything, and was always present.

To Naira, my friend since the beginning of my graduating, being always by my side.

To my lab partners and friends, especially Jean, Rina, Lidi, Regina, Dora and William for the friendship, help and the talks that made my days better.

To my “BIO2013” friends, who had accompanied me over these years, and gave my support in all tough moments.

To my “Kosmonautas” friends, that became a real important part of my life.

Thanks to entire team of the “Unidade de Crescimento de Plantas”.

To the Universidade Federal de Viçosa and Plant Physiology Graduate Program, for the opportunity to develop this work.

Also, I would like to thank all the professors of the Plant Physiology Graduate Program for the valuable teachings.

This study was partially supported by the Coordenação de Aperfeiçoamento de Pessoal de Nível Superior-Brasil (CAPES) - Finance Code 001.

Finally, I am sincerely grateful to all those who contributed for making this work possible

Thank you!

SUMMARY

ABSTRACT iv
RESUMO vi
1. INTRODUCTION 1
2. MATERIAL AND METHODS 4
2.1 Selection of *Desmonostoc* strains 4
2.2 Morphological evaluation 5
2.3 Photosynthetic evaluation 5
2.4 Growth conditions and biomass production 6
2.5 Growth curves and experimental setup 6
2.6 16S rRNA, nifD and nifH amplification, and molecular screening for cyanotoxin/protease inhibitors synthetase genes 7
2.7 Cloning and sequencing 8
2.8 Phylogenetic analyses 8
2.9 Metabolic analyzes 9
2.10 Quantification of total soluble proteins, total amino acids, phycobiliproteins and glycogen. 10
2.11 Experimental design and statistical analysis 10
3. RESULTS AND DISCUSSION 11
3.1 Sequencing and phylogenetic analysis of 16S rRNA partial gene sequences 11
3.2 NifD and nifH phylogenetic reconstructions 18
3.3 Morphological characterization 24
3.4 Photosynthetic parameters 29
3.5 Growth curves and kinetics parameters 31
3.6 Molecular screening results 35
3.7 Metabolic characterization 35
3.7.1 Chlorophyll *a* 35
3.7.2 Amino acids and total proteins 36
3.7.3 Phycobiliproteins (PBP) 37
3.5.3 Glycogen 39
3.6 PCA 40
4. CONCLUSIONS 44
5 REFFERENCES 45

ABSTRACT

ALMEIDA, Allan Victor Martins. Universidade Federal de Viçosa, July, 2019. **An integrated multi-layered analysis on *Desmonostoc.*** Advisor: Wagner Luiz Araújo. Co-advisor: Marcelo Gomes Marçal Vieira Vaz.

Cyanobacteria (phylum *Cyanobacteria*) are gram-negative bacteria, capable of performing oxygenic photosynthesis. These microorganisms form a phylogenetically coherent group despite presenting a great morphological diversity. Although the taxonomic classification of cyanobacteria was for a long time based primarily on morphological characters the application of other techniques, especially in the last decades, contributed to a better resolution of the cyanobacteria systematics, leading to a revision of the phylum. Accordingly, polyphasic approaches applied to the study of strains described as belonging to the genus *Nostoc* have indicated a polyphyletic origin of this genus, when considered its description based solely on morphological criteria. Thus, the taxonomy and systematics of strains closely related to the genus *Nostoc* have been reviewed leading to the description of new genera. Although the genus *Desmonostoc* occurs as one new genera, relatively few studies have been carried out to elucidate the phylogenetic and morphological relationships among its species, as well as between members of this genus and those closely related. In fact, only one study performed the characterization of a *Desmonostoc* strain, culminating with the description of the species *D. salinum* whereas another described the possible biotechnological application of members of this genus. In this context, the present study investigated the diversity within the genus *Desmonostoc*, based on morphological, molecular, metabolic and physiological characters. Although the last character is a non-usual tool used in the polyphasic approach it was efficient in the characterization of the genus *Desmonostoc* performed here. Our phylogenetic analysis for the 16S rRNA gene put all strains used here in the D1 cluster of *Desmonostoc* and demonstrate the possible emergence of two novel sub-clusters. It was also possible to observe that the nitrogenase genes, *nif*D and *nif*H, exhibits different evolutionary histories within the *Desmonostoc* strains. Collectively metabolic and physiological data, coupled with the morphometric ones are, in general, in good agreement with the separation based on the 16S phylogeny. Furthermore, it provide important

information on the diversity of *Desmonostoc* lineages collected from different brazilian biomes by revealing that they are cosmopolitan strains, acclimatized to low luminous intensities, with great metabolic diversity within the same genus and with biotechnological potential.

RESUMO

ALMEIDA, Allan Victor Martins. Universidade Federal de Viçosa, julho de 2019. **Uma análise integrada de multi-camadas em *Desmonostoc.*** Orientador: Wagner Luiz Araújo. Coorientador: Marcelo Gomes Marçal Vieira Vaz.

As cianobactérias (filo *Cyanobacteria*) caracterizam-se como bactérias gram-negativas, capazes de realizar fotossíntese oxigênica. Esses micro-organismos formam um grupo filogeneticamente coerente e apresentam, ainda, grande diversidade morfológica. Cumpre mencionar que a classificação taxonômica de cianobactérias foi, por muito tempo, baseada em caracteres morfológicos pouco precisos. Especialmente na última década, a aplicação de outras técnicas contribuiu para uma melhor resolução da sistemática desse filo, levando a uma revisão do grupo. Abordagens polifásicas, aplicadas aos estudos de linhagens descritas como pertencentes ao gênero *Nostoc*, têm indicado uma provável origem polifilética desse gênero, quando considerada sua descrição baseada em critérios morfológicos. Assim, a taxonomia e sistemática de linhagens próximas ao gênero *Nostoc* tem sido revisada levando à proposição de novos gêneros, dentre os quais destaca-se o gênero *Desmonostoc*. No entanto, poucos estudos foram realizados com vistas à elucidação das relações filogenéticas e morfológicas dentre suas espécies, bem como entre membros deste gênero e os proximamente relacionados. Registre-se que, até o momento, apenas um trabalho realizou a caracterização de uma linhagem de *Desmonostoc*, culminando com a descrição da espécie *D. salinum*. Ademais, apenas um trabalho descreve a possível aplicação biotecnológica de membros deste gênero. Neste contexto, o presente estudo teve como objetivos avaliar a diversidade do gênero *Desmonostoc*, baseando-se em caracteres morfológicos, moleculares, metabólicos e fisiológicos. Cabe mencionar que embora esse último caráter seja uma ferramenta pouco utilizada na abordagem polifásica, o mesmo se mostrou eficiente na caracterização e separação de linhagens do gênero *Desmonostoc*. As análises filogenéticas para o gene que codifica para o rRNA 16S indicaram o agrupamento de todas linhagens desse trabalho no *cluster* D1, indicando ainda a possível emergência de dois *sub-cluster* dentro do *cluster* D1. Também foi possível observar que os genes que codificam para o

complexo da Nitrogenase, *nif*D e *nif*H, apresentam diferentes histórias evolutivas. Tomados em conjunto, dados metabólicos e fisiológicos, juntamente com morfométricos corroboram, no geral, com a separação observada na filogenia baseada em sequências do rRNA 16S. Ademais, tais resultados forneceram informações sobre a diversidade de linhagens coletadas em diferentes biomas brasileiros, revelando que as mesmas se mostram como linhagens cosmopolitas, aclimatadas a baixas intensidades luminosas, com uma grande diversidade metabólica dentro do mesmo gênero e com potencial biotecnológico.

1. INTRODUCTION

Cyanobacteria (phylum *Cyanobacteria*) are gram-negative bacteria (*Bacteria* domain), capable of perform oxygenic photosynthesis (Smith et al., 1967). These microorganisms exhibit a great morphological diversity, ranging from unicellular to true-branch heterocytous filaments forms (Komárek & Kaštovský, 2003). Many strains also carry out the biological nitrogen fixation (BNF) (Alberto A. Esteves-Ferreira et al., 2017; Postgate, 1982), making these organisms important agents in the biogeochemical cycles of carbon (C) and nitrogen (N) (Vitousek & Howarth, 1991). Additionally, cyanobacteria exhibit a large genetic, metabolic and physiological variety, allowing these organisms to inhabit a wide range of terrestrial and aquatic environments (Schirrmeister et al., 2013).

Despite its great morphological diversity, *Cyanobacteria* form a phylogenetically coherent group (Komarek, 2006; Komárek et al., 2014). In this sense, the systematics of this phylum has been revised during the last years to better understand the evolutionary relations among the different groups (Fiore et al., 2007; Genuário et al., 2015; Gugger and Hoffmann, 2004; Hoffmann et al., 2005; Komárek et al., 2014; Korelusova et al., 2009; Vaz et al., 2015). These organisms have been classified within both Botanical and Microbiological systems of taxonomy and systematics (Baselga and Araújo, 2010; Castenholz et al., 2001). In the first case, once cyanobacteria predominantly perform oxygenic photoautotrophic metabolism, this fact would justify their inclusion in the group of “algae” (Corliss et al., 1979) and their inclusion in the International Code of Nomenclature for algae, fungi and plants (Baselga and Araújo, 2010). However, the organization of cell structure, the cell wall composition and ribosome structures, reveal the prokaryotic nature of cyanobacterial cells, justifying the positioning of this group within gram-negative bacteria (Rippka, 1988; Stanier et al., 1971) and the inclusion of the group in the International Code of Bacterial Nomenclature, covered by the *Bergey's Manual of Systematic Bacteriology* (Castenholz et al., 2001).

The taxonomic classification of cyanobacteria was for a long time based primarily on morphological characters (Taton et al., 2006). However, especially in the last two decades, the application of molecular techniques, including the

usage of the gene sequence encoding for the 16S rRNA in phylogenetic inference studies, has extensively contributed to a better resolution of cyanobacterial systematics (Komarek, 2006; Komárek, 2010a; Mai et al., 2018; Ramos et al., 2018; Silva et al., 2014). The use of other characteristics, such as ecology, life cycle and ultrastructure, has also been applied for the classification of cyanobacteria, allowing a more robust characterization named hereafter as "Polyphasic Classification" (Hoffmann et al., 2005).

Among the cyanobacterial genera, *Nostoc* was one of the first to be described (Bornet & Flahault, 1843), and is one of the most studied (Bagchi et al., 2017a; Genuário et al., 2015; Hrouzek et al., 2005; Papaefthimiou et al., 2008). This genus is recognized as the "genus-type" of both the order Nostocales and the family Nostocaceae, showing a morphology characterized by isopolar filaments, which possess vegetative as well as differentiated cells, such as heterocytes and akinetes (Komárek and Anagnostidis, 1989). In recent years, the use of the polyphasic approach in studies of strains formerly described as *Nostoc* (*Nostoc sensu lato*) have indicated a polyphyletic origin of this genus when considered its description based on morphological criteria (Hrouzek et al., 2005; Papaefthimiou et al., 2008; Silva et al., 2014). This polyphyletic origin of *Nostoc* led to the revision of the taxonomy and systematics status of strains/groups morphologically related to this genus, culminating in the description of new genera such as *Mojavia* (Řeháková et al., 2007), *Desmonostoc* (Hrouzek et al., 2013), *Halotia* (Genuário et al., 2015), *Komarekiella* (Hentschke et al., 2017), *Aliinostoc* (Bagchi et al., 2017a), *Compactonostoc* (Cai et al., 2019b) and *Minunostoc* (Cai et al., 2019a).

Phylogenetic analyzes based on 16S rRNA sequences obtained from members of the genus *Desmonostoc* indicate that these sequences are grouped into two internal clusters (Hrouzek et al., 2013). One of these clusters, called D2, harbors the sequence of the type-species (reference strain), "*Desmonostoc muscorum* NIVA-CYA 817 (AJ630451)" whereas the cluster D1 aggregates sequences from other *Desmonostoc* spp. This fact apart, since the description of the genus *Desmonostoc* relatively few studies have been carried out aiming to elucidate the phylogenetic and morphological relationships among its species, as well as between members of this genus and the closely related ones (Cai et al., 2018; de Alvarenga et al., 2018; Miscoe et al., 2016;

Obuekwe et al., 2019; Saraf et al., 2018). To our knowledge, only one study was focused on the physiological and metabolic characterization of a *Desmonostoc* strain, culminating with the description of *D. salinum* (de Alvarenga et al., 2018). In addition another study described the possible biotechnological application of members of this genus (Sanz et al., 2015); and, recently, *Desmonostoc* strains isolated from Brazilian environments were described (Obuekwe et al., 2019).

Although it is by far the most used, the use of solely 16S rRNA sequences as marker for molecular phylogeny studies has been recently discussed (Bolhuis et al., 2010; A.A. Esteves-Ferreira et al., 2017; Henson et al., 2004; Tamas et al., 2000), since some issues arose from lower hierarchical levels of analysis, as trifurcations or polytomies. Accordingly, the use of other molecular markers, such as *rpo*C1 (Fergusson & Saint, 2000), which encodes the β-subunit of RNA polymerase, and *nif*H (Alberto A. Esteves-Ferreira et al., 2017; Genuário et al., 2013; Zehr et al., 1997), which encodes for the enzyme dinitrogenase reductase from the enzymatic complex of Nitrogenase, has aided in the resolution of some groups, even though at other hierarchical levels, mainly species or corroborating infra diversity at generic level (Tamas et al., 2000).

Ecophysiological characteristics of cyanobacteria, as facultative photoheterotrophic growth, synthesis of some pigments, or requirement of vitamin B12 (Rosmarie Rippka et al., 1979), can be also used in polyphasic studies (Komárek, 2010b), and the use of characteristics such as life cycle, can provide a more robust phenotypical and ecological characterization (Mateo et al., 2011). For instance, formation of hormogonia and akinetes that occurs as part of the nostocacean life cycle (R. Rippka et al., 1979a), being the hormogonia defined as short sections of trichomes, separated from the original trichome, with reproductive purposes (Komárek and Kaštovský, 2003) can be useful in polyphasic studies. These short trichomes lack heterocytes and display some of the following properties: gliding motility, smaller cell size, and different cell shape in comparison with vegetative cells and filaments (Rosmarie Rippka et al., 1979). As consequence, the life cycle of *Nostoc* is complex and an important taxonomic feature (ANAGNOSTIDIS, 1985) that must be considered.

In addition to issues related to either taxonomy or phylogeny, cyanobacteria appear as potential organisms for use in industrial and biotechnological applications, as they exhibit rapid cell growth, basic nutritional requirements (mainly light, water and CO_2), as well as they are naturally transformable, thus presenting potential to be used in genetic engineering (Eduardo et al., 2016; Mashayekhi et al., 2017). Due to their great metabolic diversity and simple nutritional requirements and plasticity, the use of cyanobacteria in areas unsuitable for agriculture is viable for the production of biomass for biofuels and other bioproducts (Mashayekhi et al., 2017; Sciuto & Moro, 2015). Regardless the applied purposes it is mandatory, however, to enhance our knowledge regarding the diversity of the cyanobacteria from not only taxonomic but also from a metabolic and physiological point of view. It seems reasonable to posit that systematics enable the understanding of the evolutionary history of these organisms, and gives an idea of local species. Thus, allowing us to distinguish the endemic species or genera existing in a given area. However, despite the significance of physiological characters , relatively few studies have focused in these traits (de Alvarenga et al., 2018; Genuário et al., 2015). .

To date, no detailed study has been carried out aiming to characterize the molecular and metabolic diversity of *Desmonostoc* strains. Thus, to elucidate the diversity of *Desmonostoc* strains from distinct environments, here a set of strains were characterized based on morphologic, molecular, ecological as well as metabolic and physiological traits. Taken together, the metabolic and physiological data coupled with the morphometric data obtained demonstrate a good agreement with the separation based solely on the 16S phylogeny. Furthermore, the usage of metabolic and physiological traits, despite being a non-usual tool for the polyphasic approach for description of novel taxa, presents itself as highly helpfully in the proposal of new species.

2. MATERIAL AND METHODS

2.1 Selection of *Desmonostoc* strains

The Collection of Cyanobacteria and Microalgae (CCM-UFV) harbors a

total of sixty-three cyanobacterial strains, of which 47 belong to the order Nostocales (filamentous heterocytous morphotypes). From them, 33 belong to the Nostocaceae family, and 26 have morphological traits related to *Nostoc sensu lato* (*Nostoc*-like). Although strains belonging to the genus *Desmonostoc* can be differentiated based on morphological characters, the phylogeny based on 16S rRNA sequences was further applied for a correct identification. In this way, 19 strains were identified as *Desmonostoc* spp. (Table 1), which were further analyzed here.

2.2 Morphological evaluation

For morphological evaluation, aliquots of each *Desmonostoc* strain were collected during the logarithmic (log) phase (2 to 5-old day cultures). Morphological observations were conducted using a Zeiss Axioskop 40 optical light microscope equipped with an AxioVision LE 4.6 digital imaging system (Carl Zeiss). The isolated strains were morphologically characterized using diacritical features (length and width of vegetative cells as well as of heterocytes, akinetes and hormogonia) according to the systematic scheme proposed previously (Komárek et al., 2014), as well as recent studies dealing with the description of novel *Desmonostoc* species and its diversity (CAI et al., 2018; de Alvarenga et al., 2018; Obuekwe et al., 2019; Saraf et al., 2018). In addition, the macroscopic appearance of the colonies was also recorded.

2.3 Photosynthetic evaluation

For the determination of the light intensity to be applied during the experiments, physiological evaluations were performed using cultures harvested when the strains reached mid-logarithmic phase (3-5 days). Cultures of each strain was individually grown in Erlenmeyer flasks (50 mL volume) containing 20 mL of BG-11_0 (Rippka et al. 1979), and maintained under light intensity of 50 μmol·photons·m^{-2}·s^{-1}, photoperiod of 16/8 h (light/dark), temperature of 24 ± 2 °C, and stirring at 100 rpm. For each strain, three technical replicates were analyzed.

To obtain the compensation and saturation points, light curves were performed for all selected strains. These parameters were measured using a

Clark-type electrode connected to a biological oxygen monitor (Chlorolab 2 System, Hansatech, Norfolk, UK), as previously described (Jeon et al., 2006; Torzillo et al., 1998), using a Clark electrode (Oxygen Monitoring System, Oxylab + Hansatec).

Briefly, the instrument was calibrated using a solution of sodium dithionite to set 0 % saturation, and after washed with distilled water. Then, 2 mL of culture with $O.D._{750nm}$ of ~ 0.5 was placed in the electrode chamber and curves of oxygen consumption and evolution, in response to photosynthetically active radiation (PAR), were performed at 25 °C by increasing the PAR intensities from 0 to 30, 40, 50, 60, 70, 80, 90 100, 150 and 200 µmol photons $m^{-2} \cdot s^{-1}$, lasting five minutes each step. Both the compensation irradiance (I_c) and saturation irradiance (I_s) were calculated according to (Xu et al. 2012).

2.4 Growth conditions and biomass production

Stock cultures of each strain were cultured in Erlenmeyer flasks (125 mL) containing 50 mL of BG-11_0 culture medium, which were kept under photoautotrophic conditions: photoperiod of 16/8 h (light/dark), applying the light intensities of 60 µmol photons$\cdot m^{-2} \cdot s^{-1}$, at 25 ± 2°C. For inoculum production, 1 mL aliquots were taken from stock cultures of each strain and inoculated in Erlenmeyer flasks (500 mL) containing 200 mL of BG-11_0 medium. The flasks were kept under the photoautotrophic conditions described above, excepted by the light intensity, which was selected according to the response curve of PAR, determined above (item 2.3), during ~10 days.

2.5 Growth curves and experimental setup

To identify the growth phases (lag, log, linear and stationary), growth curves were performed for eight strains, which were selected considering the phylogenetic grouping inferred from the phylogenetic reconstruction based on 16S rRNA sequences (Figure 1). The experiments were carried out in Erlenmeyer flasks (50 mL) filled with 20 mL of BG-11_0 medium applying an initial cell density corresponding to an optical density of 0.1 under the light wavelength of 750 nm (OD_{750nm} ~ 0.1). These growth curves were conducted with 3 replicates (n = 3), during 14 days, totalizing 15 sample points. Growth

was evaluated by optical density determination and dry mass, which were measured at intervals of 24 h.

Next, another round of curves were performed, which were conducted with 4 replicates (n = 4) using Erlenmeyer flasks (125 mL) filled with 50 mL of BG-11_0 medium, up to early-to-mid-stationary phase. At this point the total biomass was collected, being centrifuged (10,000 rpm, 10 minutes, room temperature) and freeze-dried. The obtained biomasses of each strain were used for metabolic analysis as described below.

2.6 16S rRNA, *nif*D and *nif*H amplification, and molecular screening for cyanotoxin/protease inhibitors synthetase genes

The total genomic DNA of all 19 *Desmonostoc* strains was extracted from 3 mL of culture in exponential phase of growth. Cells were concentrated by centrifugation at 10,000 × g, 10 minutes, room temperature; the supernatant was discarded and the pellet was extracted using the UltraClean® Microbial DNA Isolation Kit (MoBio, Carlsbad, CA).

The 16S rRNA plus the ITS 16-23S region was amplified from the genomic DNAs by PCR using the oligonucleotide primers 27F1 (Neilan et al., 1997) and 23S30R (Taton et al., 2003). Amplification was performed following the steps described by (Genuário et al., 2013).

Partial *nif*D and *nif*H sequences were also amplified applying the primers nifD552-F/nifD861-R (Roeselers et al., 2007) and NifH_Olson_F/NifH_Olson_R (Olson et al., 1998), following the conditions described in the cited references.

The molecular screening for microcystin (*mcy*D, *mcy*E and *mcy*G) and saxitoxin (*sxt*A, *sxt*B and *sxt*I) was conducted using the primers designed by Hoff-Risseti et al. (2013) and Rantala et al. (2004), respectively. The reaction and cycling conditions for microcystin and saxitoxin PCR screening were performed as described by Genuário et al. (2013) and Rantala et al. (2004), respectively.

Investigation of the genetic potential for microviridin (protease inhibitor) production was conducted by the screening of the *mdn*A gene, as described by Cadel-Six et al. (2008).

2.7 Cloning and sequencing

The PCR products spanning the expected length were cloned in a pGEM-T Easy Vector System (Promega, Madison, WI, USA) according to the manufacturer's manual. Ultra-competent *Escherichia coli* DH5α cells were transformed and recombinant plasmids were purified from white colonies, using the UltraClean® Standard Mini Plasmid Prep Kit (MoBio, Carlsbad, CA). Plasmids containing the expected fragments were sequenced using the vector's M13F/R primer set. In addition, for complete sequencing of the 16S rRNA plus ITS 16-23S sequences, internal primer sets 341-357F/R, 685-704F/R and 1099-1114F/R were used (Genuário et al., 2013). The sequenced fragments were assembled into one contig using the software Phred/Phrap/Consed (Philip Green, Univ. of Washington, Seattle, USA) and only bases with>20 quality were considered.

2.8 Phylogenetic analyses

The sequences generated in this study were compared with those previously deposited in GenBank, from the National Center for Biotechnology Information (NCBI), using the Basic Local Alignment Search Tool (BLAST) (Altschul et al., 1990).

The 16S rRNA gene sequences generated in this study and related ones retrieved from GenBank (NCBI) were used to construct a phylogenetic tree comprising sequences from heterocytous (Nostocales) strains. A total of 134 sequences was aligned using *CLUSTAL W*, trimmed (matrix with a 1,454-bp length) and used to infer the phylogeny based on the Maximum Likelihood (ML) method, applying the MEGA package version 5 (Tamura et al., 2011). The Kimura 2-parameter model of substitution with gamma distribution and with an estimate of proportion of invariable sites (K2+G+I) was selected as the best fitting model, applying the jModelTest 2.1.1 (Darriba et al., 2012). The robustness of the phylogenetic trees was estimated by bootstrap analysis using 1,000 replications.

For the phylogenetic analysis based on partial *nif*D gene sequences, those obtained in this study and related ones retrieved from GenBank were used. Ninety-five sequences were aligned using *CLUSTAL W*, trimmed (matrix

with a 321-bp length) and used to infer the phylogeny based on the Maximum Likelihood (ML) method, applying the MEGA package version 5 (Tamura et al., 2011). The Kimura 2-parameter model of substitution with gamma distribution (K2+G) was selected as the best fitting model, applying the model testing function in MEGA version 5 (Tamura et al., 2011). The robustness of the phylogenetic trees was estimated by bootstrap analysis using 1,000 replications.

For the phylogenetic analysis based on partial *nif*H gene sequences, those obtained in this study and related ones retrieved from GenBank were used. Seventy-six sequences were aligned using CLUSTAL W, trimmed (matrix with a 417-bp length) and used to infer the phylogeny based on the Maximum Likelihood (ML) method, applying the MEGA package version 5 (Tamura et al., 2011). The Kimura 2-parameter model of substitution with gamma distribution (K2+G) was selected as the best fitting model, applying the model testing function in MEGA version 5 (Tamura et al., 2011). The robustness of the phylogenetic trees was estimated by bootstrap analysis using 1,000 replications.

2.9 Metabolic analyzes

For the metabolic analyzes the freeze-dried biomass obtained from the early-to-mid-stationary phase (item 2.5) was used. In a first step, a total of 700 µL of methanol (100 %) was added to the microtubes containing the pellets (pre weighted) of each strain. The samples were submitted to 5 cycles of freezing and thawing using liquid nitrogen and hot water. After these cycles, the samples were incubated for 20 minutes at 80 °C under constant stirring at 500 rpm. Then, the samples were centrifuged at 13,500 rpm for 10 minutes at 4 °C. The supernatant (600 ~ 650 µL) was collected and stored in a new 1.5 mL microtube. The pellet was used to extract total soluble proteins and glycogen, while the supernatant was used to quantify chlorophyll *a*, soluble sugars and amino acids. The chlorophyll *a* concentration was determined spectrophotometrically immediately after extraction from the separated supernatant, the absorbance being determined at 665 nm (Porra et al., 1989).

2.10 Quantification of total soluble proteins, total amino acids, phycobiliproteins and glycogen.

To the residual supernatant from the previous step were added 375 µL of chloroform and 750 µL of water. The material was centrifuged at 13,500 rpm for 10 minutes at 4 °C, giving rise to two very characteristic phases: one aqueous (polar, upper) and one organic (apolar and lower). The aqueous phase, in which the metabolites of interest are found, was collected and transferred to another microtube for further analysis. The pellet was washed with 1,000 µL of ethanol (70 % v/v), treated with 0.1 M NaOH and heated for one hour at 95 °C for protein extraction and then neutralized with 1 M acetic acid for quantification of glycogen. Quantification of total amino acids was performed as described by Cross et al. (2006); the glycogen content was determined using a modified protocol for extraction and quantification of starch (Fernie et al., 2001) and the content of total soluble proteins was determined was previously described (Bradford, 1976).

For extraction of the phycobiliproteins (PBP), 5 mg of freeze-dried biomass were submitted to a tissue lyzer (Retsch, MM400) for two rounds of 2 minutes each, on a frequency of 24 Hz. Then, 5 mL of Sodium Acetate Buffer were added to this biomass and centrifuged at 13,500 rpm for 10 minutes. From the supernatant, 1,9 mL was collected and transferred to a new tube, where 100 µL of streptomycin sulfate (200 $mg \cdot mL^{-1}$) was added, and centrifuged in the same conditions of the previous step. Then, 1.4 mL of the supernatant was transferred to a new tube, and 400 µL of dithiothreitol (DDT) 1mM was added. The contents of phycobiliproteins were quantified based on spectrophotometry as described by de Marsac and Houmard (1988).

2.11 Experimental design and statistical analysis

The experiment was conducted and analyzed following a randomized block design with each block composed of 19 strains with at least three replications. The data obtained for growth, physiological and metabolic parameters were subjected to an analysis of variance (ANOVA, $P<0,05$), and the means were compared using the Tukey's test at 5 % probability. All analyses were performed on STATISTICA software (StatSoft). The Principal

Component Analysis (PCA) and Clustering was performed on R 3.6.1 software, with the libraries gplots, ggplot2, ggfortify and factoextra.

3. RESULTS AND DISCUSSION

3.1 Sequencing and phylogenetic analysis of 16S rRNA partial gene sequences

Taking into consideration the sampling site (ecological and geographical traits), the majority of the strains used here were isolated from freshwater samples (Table 1). However a number of *Desmonostoc* strains have been reported from terrestrial environments, mainly soils (Hrouzek et al., 2013) as well as wet rocky wall (CAI et al., 2018). Nevertheless, in this study, strains from harsh environments, ranging from sediments of gold mining areas (CCM-UFV069 and 070) (Obuekwe et al., 2019) as well as from a saline-alkaline lake (Laguna Amarga) (*D. salinum* CCM-UFV059) (de Alvarenga et al., 2018) were also isolated and studied. Other exceptions are the strains CCM-UFV002 and CCM-UFV054, which were collected from soil and epiphytic biofilm, respectively. It is important to mention, however, that ecological traits are seemingly not able to help solving the systematics of *Desmonostoc*, as previously discussed (Hrouzek et al., 2013; Obuekwe et al., 2019).

All studied *Desmonostoc* spp. (19 strains) had their 16S rRNA partial gene sequences successfully sequenced. The length of these sequences ranged from 1,400 to 1,500 bp, showing identities values ≥ 99.4% when compared with available *Desmonostoc* sequences (Table 1). Notably, only the sequences retrieved from the strains *Desmonostoc* spp. CCM-UFV018, CCM-UFV054, CCM-UFV069 and CCM-UFV070 showed identity values ≤ 99% (Table 1). Accordingly, the strain CCM-UFV059 was recently described as a new species, named *D. salinum* (de Alvarenga et al., 2018), whilst the strains CCM-UFV069 and CCM-UFV070 were recently characterized in terms of morphology and molecular phylogeny (Obuekwe et al., 2019).

Given the phylogenetic reconstruction based on 16S rRNA, all sequences generated in this study were harbored in the type *Desmonostoc* cluster (Figure 1), according to previous reports (de Alvarenga et al., 2018; Hrouzek et al., 2013; Obuekwe et al., 2019). In good agreement with previous

results (Hrouzek et al. 2013), we also observed an already described topology, in which the *Desmonostoc* cluster shows two subdivisions namely D1 and D2 sub-clusters. More importantly, the genus *Desmonostoc* seems to be robust in terms of molecular phylogeny, reinforcing previous results from independent studies (Bagchi et al., 2017b; Cai et al., 2019b; de Alvarenga et al., 2018; Hrouzek et al., 2013, 2009; Obuekwe et al., 2019; Saraf et al., 2018).

All *Desmonostoc* spp. used here were grouped in the sub-cluster D1 (Figure 1), while the sub-cluster D2 harbors, among others, the sequence from *D. muscorum* Lukesova 1/87 (AM711523), which is related to the type-species (*D. muscorum* NIVA-CYA818). To proceed with the remaining analyzes, the sub-cluster D1 was subdivided in two novel groups, one phylogenetic coherent, and one artificial (with the remaining sequences that was not grouped in the first cluster) named here as A and B, respectively (Figure 1). The majority of the *Desmonostoc* strains from CCM-UFV were grouped in the cluster A (bootstrap of 64%), being related to *D. salinum* CCM-UFV059 (de Alvarenga et al., 2018). Despite the phylogenetic relatedness among these sequences, no clear relation was observed considering their ecological or geographical origins (Table 1). The sequences of the strains *Desmonostoc* spp. CCM-UFV018, CCM-UFV054, CCM-UFV069 and CCM-UFV 070 were grouped into cluster B and showed identity values ≤98.5% to those of the type-species and other already descript species, as *D. salinum* and *D. danxiaense* (Cai et al., 2018; de Alvarenga et al., 2018). Taken together, this date coupled with our metabolic and physiological data, which will be further presented and explored, suggest that the cluster D1 harbors a group of highly diverse strains.

A threshold of 97.5 % of 16S rRNA gene identity has been suggested to separate bacteria species (Stackebrandt & Goebel, 1994) on the basis of the fact that when two strains have genetic identity below 97.5 % a value of DNA-DNA hybridization below 70 % is expected, criteria used for recognizing bacterial species (Wayne et al. 1987). This fact apart, the *Desmonostoc* spp. strains available at CCM-UFV and used here did not show identity values below 97.5%. It is important to mention that Erko Stackebrandt and Ebers (2006) suggested a change from 97.0 to 98.7–99.0% 16S rRNA gene sequence similarity for the threshold to separate species. This proposal is highly relevant to our study, since our strains (specifically CCM-UFV018, 054,

069 and 070) shown identity between 98% and 99% with the others deposited sequences, retrieved from already described species. It seems also evident that different stable phenotypes of some cyanobacteria are not reflected in 16S rRNA gene sequence comparisons (Mateo et al., 2011). This has been reported for *Merismopedia*-like isolates (Palinska et al., 1996), *Microcystis* strains (Otsuka et al., 1999) and *Leptolyngbya* spp. (Casamatta et al., 2005). This, together with the data obtained here, leads to the possibility of describing new *Desmonostoc* species.

Table 1. Codes, isolation source and identity percentage of 16S rRNA gene sequences from selected *Desmonostoc* strains compared to those deposited in GenBank.

Strain	Sampling Site (Location)	Lenght(bp)	Most related organism on GenBank (access number)	C(%)*	I(%)**
CCM-UFV002	Soil sample (Santa Bárbara-MG)	1415	Uncultured bacterium clone JFR0702_jaa51e01 (HM780037)	99	99.59
			Nostoc sp. PCC9231 (AY742452)	99	99.52
			Nostoc sp. SAG 34.92 (KM019925)	98	99.72
			Nostoc sp. 8964:3(AM711541)	98	99.72
			Nostoc entophytum IAM M-267 (AB093490)	98	99.65
CCM-UFV003	Water bodies and sediment from gold mine (Paracatu-MG)	1416	Uncultured bacterium clone JFR0702_jaa51e01 (HM780037)	99	99.45
			Nostoc sp. SAG 34.92 (KM019925)	98	99.72
			Nostoc sp. 8964:3(AM711541)	98	99.72
			Nostoc sp. PCC9231 (AY742452)	99	99.45
			Nostoc entophytum IAM M-267 (AB093490)	98	99.65
CCM-UFV004	Water bodies and sediment from gold mine (Paracatu-MG)	1415	Uncultured bacterium clone JFR0702_jaa51e01 (HM780037)	99	99.59
			Nostoc sp. PCC9231 (AY742452)	99	99.52
			Nostoc sp. SAG 34.92 (KM019925)	98	99.72
			Nostoc sp. 8964:3(AM711541)	98	99.72
			Desmonostoc salinum CCM-UFV059 (KX787933)	98	99.58
CCM-UFV005	Water bodies and sediment from gold mine (Paracatu-MG)	1417	Uncultured bacterium clone JFR0702_jaa51e01 (HM780037)	99	99.45
			Nostoc sp. PCC9231 (AY742452)	99	99.52
			Nostoc sp. SAG 34.92 (KM019925)	98	99.65
			Nostoc sp. 8964:3(AM711541)	98	99.65
			Nostoc entophytum IAM M-267 (AB093490)	98	99.58
CCM-UFV009	Water bodies and sediment from gold mine (Paracatu-MG)	1415	Uncultured bacterium clone JFR0702_jaa51e01 (HM780037)	99	99.59
			Nostoc sp. PCC9231 (AY742452)	99	99.52

			Nostoc sp. SAG 34.92 (KM019925)	98	99.72
			Nostoc sp. 8964:3(AM711541)	98	99.72
			Nostoc entophytum IAM M-267 (AB093490)	98	99.65
CCM-UFV011	Turvo Sujo River (Viçosa-MG)	1414	Uncultured bacterium clone JFR0702_jaa51e01 (HM780037)	99	99.72
			Nostoc sp. PCC9231 (AY742452)	99	99.65
			Nostoc sp. SAG 34.92 (KM019925)	98	99.86
			Nostoc sp. 8964:3(AM711541)	98	99.86
			Nostoc entophytum IAM M-267 (AB093490)	98	99.79
CCM-UFV012	Turvo Sujo River (Viçosa-MG)	1414	Uncultured bacterium clone JFR0702_jaa51e01 (HM780037)	99	99.79
			Nostoc sp. PCC9231 (AY742452)	99	99.72
			Nostoc sp. SAG 34.92 (KM019925)	98	99.93
			Nostoc sp. 8964:3(AM711541)	98	99.93
			Nostoc entophytum IAM M-267 (AB093490)	98	99.86
CCM-UFV013	Turvo Sujo River (Viçosa-MG)	1415	Uncultured bacterium clone JFR0702_jaa51e01 (HM780037)	99	99.59
			Nostoc sp. SAG 34.92 (KM019925)	98	99.79
			Nostoc sp. 8964:3(AM711541*)*	98	99.79
			Nostoc sp. PCC9231 (AY742452)	99	99.52
			Nostoc entophytum IAM M-267 (AB093490)	98	99.72
CCM-UFV014	Turvo Sujo River (Viçosa-MG)	1414	Uncultured bacterium clone JFR0702_jaa51e01 (HM780037)	99	99.79
			Nostoc sp. PCC9231 (AY742452)	99	99.72
			Nostoc sp. SAG 34.92 (KM019925)	98	99.93
			Nostoc sp. 8964:3(AM711541)	98	99.93
			Nostoc entophytum IAM M-267 (AB093490)	98	99.86
CCM-UFV018	Do Carmo River, Ribeirão do Funil (Ouro Preto-MG)	1414	*Nostoc muscorum* CCAP 1453/22 (HF678509)	99	98.96
			Nostoc linckia NIES-25 (AP018222)	100	99.76
			Desmonostoc sp. SA25 (MF642333)	99	98.89
			Nostoc sp. Cr4 (AM711533)	98	99.02

			Desmonostoc danxiaense CHAB5869 (MH291267)	100	98.89
CCM-UFV020	Do Carmo River, Ribeirão do Funil (Ouro Preto-MG)	1414	Uncultured bacterium clone JFR0702_jaa51e01 (HM780037)	99	99.72
			Nostoc sp. PCC9231 (AY742452)	99	99.65
			Nostoc sp. SAG 34.92 (KM019925)	98	99.86
			Nostoc sp. 8964:3(AM711541)	98	99.86
			Nostoc entophytum IAM M-267 (AB093490)	98	99.79
CCM-UFV022	Do Carmo River, Ribeirão do Funil (Ouro Preto-MG)	1413	Uncultured bacterium clone JFR0702_jaa51e01 (HM780037)	99	99.45
			Nostoc sp. SAG 34.92 (KM019925)	98	99.65
			Nostoc sp. 8964:3(AM711541)	98	99.65
			Nostoc sp. PCC9231 (AY742452)	99	99.38
			Nostoc entophytum IAM M-267 (AB093490)	98	99.58
CCM-UFV028	Carangola River (Carangola-MG)	1414	Uncultured bacterium clone JFR0702_jaa51e01 (HM780037)	99	99.72
			Nostoc sp. PCC9231 (AY742452)	99	99.65
			Nostoc sp. SAG 34.92 (KM019925)	98	99.86
			Nostoc sp. 8964:3(AM711541)	98	99.86
			Nostoc entophytum IAM M-267 (AB093490)	98	99.79
CCM-UFV029	Carangola River (Carangola-MG)	1414	Uncultured bacterium clone JFR0702_jaa51e01 (HM780037)	99	99.72
			Nostoc sp. PCC9231 (AY742452)	99	99.65
			Nostoc sp. SAG 34.92 (KM019925)	98	99.86
			Nostoc sp. 8964:3(AM711541)	98	99.86
			Nostoc entophytum IAM M-267 (AB093490)	98	99.79
CCM-UFV031	Carangola River (Carangola-MG)	1414	Uncultured bacterium clone JFR0702_jaa51e01 (HM780037)	99	99.65
			Nostoc sp. SAG 34.92 (KM019925)	98	99.86
			Nostoc sp. 8964:3(AM711541)	98	99.86
			Nostoc sp. PCC9231 (AY742452)	99	99.59
			Nostoc entophytum IAM M-267 (AB093490)	98	99.79
CCM-UFV054	Tree surface (innacurate)	1413	*Nostoc muscorum* CCAP 1453/22 (HF678509)	99	98.9

			Nostoc linckia NIES-25 (AP018222)	100	98.69
			Desmonostoc sp. SA25 (MF642333)	99	98.89
			Nostoc sp. Cr4 (AM711533)	98	99.02
			Nostoc sp. PCC7906 (AB320958)	98	98.89
CCM-UFV059	Laguna Amarga Pound (Torres Del Paine-Chile)	1414	*Nostoc* sp. SAG 34.92 (KM019925)	100	99.86
			Nostoc sp. 8964:3 (AM711541)	100	99.86
			Nostoc entophytum IAM M-267 (AB093490)	100	99.79
			Nostoc sp. PCC9231 (AY742452)	99	99.72
			Desmonostoc sp. PCC 8306 (HG004584)	100	99.65
CCM-UFV069	Water bodies and sediment from gold mine (Paracatu-MG)	1417	*Nostoc* sp. PCC 7906 (AB320958)	100	98.24
			Desmonostoc sp. CCIBT 3489 (KX638490)	100	98.24
			Desmonostoc sp. PCC7422 (HG004586)	100	98.17
			Desmonostoc sp. SA25 (MF642333)	100	98.10
			Desmonostoc sp. CENA365 (KR137586)	100	98.10
CCM-UFV070	Water bodies and sediment from gold mine (Paracatu-MG)	1415	*Desmonostoc* sp. PCC8107 (HG004583)	100	98.87
			Nostoc linckia NIES-25 (AP018222)	100	98.66
			Desmonostoc sp. PCC8306 (HG004584)	100	98.59
			Desmonostoc sp. SA14 (MF642332)	100	98.59
			Nostoc sp. CACIAM 19 (MG272378)	100	98.45

*Coverage **Identity

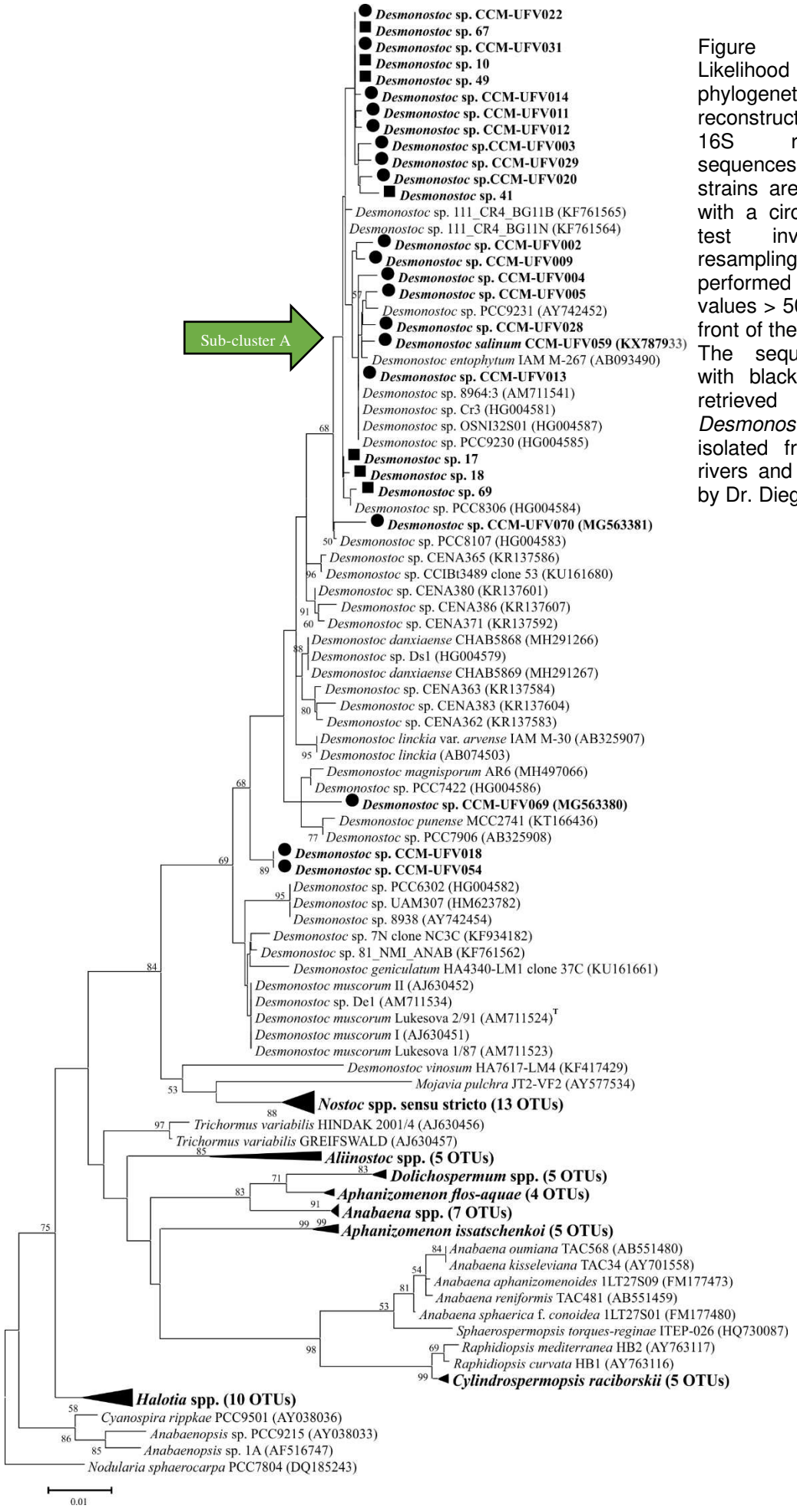

Figure 1. Maximum Likelihood (ML) phylogenetic reconstruction based on 16S rRNA gene sequences. The studied strains are shown in bold with a circle. A bootstrap test involving 1,000 resamplings was performed and bootstrap values > 50 % are given in front of the relevant nodes. The sequences marked with black squares were retrieved from *Desmonostoc* strains isolated from Amazonian rivers and kindly provided by Dr. Diego B. Genuário.

3.2 *nif*D and *nif*H phylogenetic reconstructions

In addition to the phylogenetic analysis based on 16S rRNA gene sequences, phylogenetic inferences based on *nif*D and *nif*H partial nucleotide sequences were also carried out (Figure 2 and 3). Studies dealing with the taxonomy and systematics of *Desmonostoc* strains applying *nif* sequences are, to date, absent and have predominantly focused on the 16S Rrna sequences (CAI et al., 2018; de Alvarenga et al., 2018; Obuekwe et al., 2019; Saraf et al., 2018). Nevertheless, unpublished *nif*H sequences obtained from putative *Desmonostoc* strains (from CENA Culture Collection) are deposited at GenBank (NCBI), and were used in the presented phylogenetic analysis (Figure 2).

Considering the topology based on *nif*D sequences, all *Desmonostoc* strains were grouped together (bootstrap of 81 %) (Figure 2), in a similar pattern as found for 16S rRNA-based phylogeny (Figure 1). The most related sequence to the "*Desmonostoc*" group was that retrieved from *Nostoc linckia* NIES-25 (AP01822). It is important to mention that this strain (NIES-25), besides being identified as *"Nostoc*", shares high 16S rRNA identity with some of *Desmonostoc* CCM-UFV strains (Table 1). It seems reasonable, therefore, to assume that the strain NIES-25 belongs to the genus *Desmonostoc*. Together, these results indicate that *nif*D most likely has a similar evolutionary history, compared to 16S rRNA gene sequences.

The topology observed in the *nif*H-based phylogenetic tree (Figure 3) did not correlated with that obtained for both, 16S rRNA and *nif*D gene sequences. Interestingly, the novel *nif*H sequences, retrieved from our *Desmonostoc* strains, were spread into three different clusters (Figure 3). In one of them, the *nif*H sequences of CCM-UFV004, CCM-UFV009, CCM-UFV011, CCM-UFV013, CCM-UFV020 and CCM-UFV028 grouped with a sequence retrieved from an uncultured clone and with the sequence from *Desmonostoc* sp. CENA365. Another sub-cluster harboring the *nif*H sequences from CCM-UFV002, CCM-UFV059 and CCM-UFV070 was also observed, which was more related with sequences from *Nostoc* (Nostocaceae), *Tolypothrix* and *Fremyella* (both, Tolypothrichaceae). This last sub-cluster harbored sequences of strains belonging to the sub-cluster A and

B (Figure 1). The *nif*H sequence from CCM-UFV054 was placed as an orphan branch, closely related to sequences taken from *Desmonostoc* strains as well as from other nostocacean genera (*Nostoc* and *Nodularia*). Even though the topology of *nif*H-based phylogenetic reconstruction did not showed any apparent relation with either 16S rRNA or *nif*D phylogenetic trees, some interesting results for sub-cluster B were observed as it can be depicted from the presence of the CCM-UFV054 in a distinct singular phylogenetic position, whereas CCM-UFV070 belongs to the same group of some strains harbored in sub-cluster A.

Phylogenetic reconstructions based on *nif*D and 16S rRNA sequences showing similar pattern of grouping have been observed, at least for higher taxonomic groups, such as orders and families (Alberto A. Esteves-Ferreira et al., 2017; Henson et al., 2004). As observed in Figure 2A, some generic and specific groups are coherent considering *nif*H, such as *Scytonema hyalinum* and *Brasilonema* (Scytonemataceae), *Hassallia* (Tolypothrichaceae), as well as *Desmonostoc* (Nostocaceae). However, for other well-stablished genera, such as *Nodularia*, *Cylindrospermum*, *Nostoc*, which comprise heterocytous-forming morphotypes, as well as *Leptolyngbya* (filamentous homocytous), *Xenococcus* and *Chroococcidiopsis* (unicellular types), there is a distinctive distribution of its members over the phylogenetic reconstruction (Figure 3).

The analysis of *nif*H phylogenetic history has shown controversial patterns for two nostocacean genera for which this molecular marker was applied. Accordingly, for the genus *Hydrocoryne*, a similar topology between 16S rRNA and nif*H*-based trees was observed (Genuário et al., 2013). However, considering the genus *Halotia*, while the 16S rRNA sequences formed a single robust cluster, the *nif*H sequences were spread into three sub-groups (Genuário et al., 2015). It seems reasonable to suggest that the phylogeny of *nif* genes seems to reflect its own evolution and not the evolutionary relationships of the organisms in which they are found (Bolhuis et al., 2010; Genuário et al., 2015). Taken together, our results shed light and add further controversy on the hypothesis regarding the evolutionary history of "Nitrogenase-genes" (*e.g, nif*D, *nif*H and *nif*K) and their value as appropriate molecular markers for genera delimitation.

Remarkably, the achievement of *nif* genes, suggesting a common ancestral, from which all cyanobacterial *nif* genes were inherited (vertical gene transfer) has been discussed elsewhere (Alberto A. Esteves-Ferreira et al., 2017; Zehr et al., 1997; Zehr and Turner, 2001). However, it has also been demonstrated that the gene cluster involved in nitrogen fixation is most likely not distributed universally among the members of the phylum *Cyanobacteria*, and as such the processes driving their dispersion and maintenance in different cyanobacterial lineages remains rather unknown (Bolhuis et al., 2010; Genuário et al., 2015). In addition, horizontal gene transfer (HGT) can explain, at least partially, the diversity of *nif*-genes found for cyanobacteria (Bolhuis et al., 2010; Roeselers et al., 2007; Stal, 2015). Considering our data, and in good agreement with previous studies (Genuário et al. 2015), incongruence between the *nif*H and 16S rRNA gene phylogenies would be thus expected . Collectively, our data indicates that *nif*D and *nif*H have different evolutionary histories, as demonstrated by the distinct tree topologies, and are in consonance with the HGT theory.

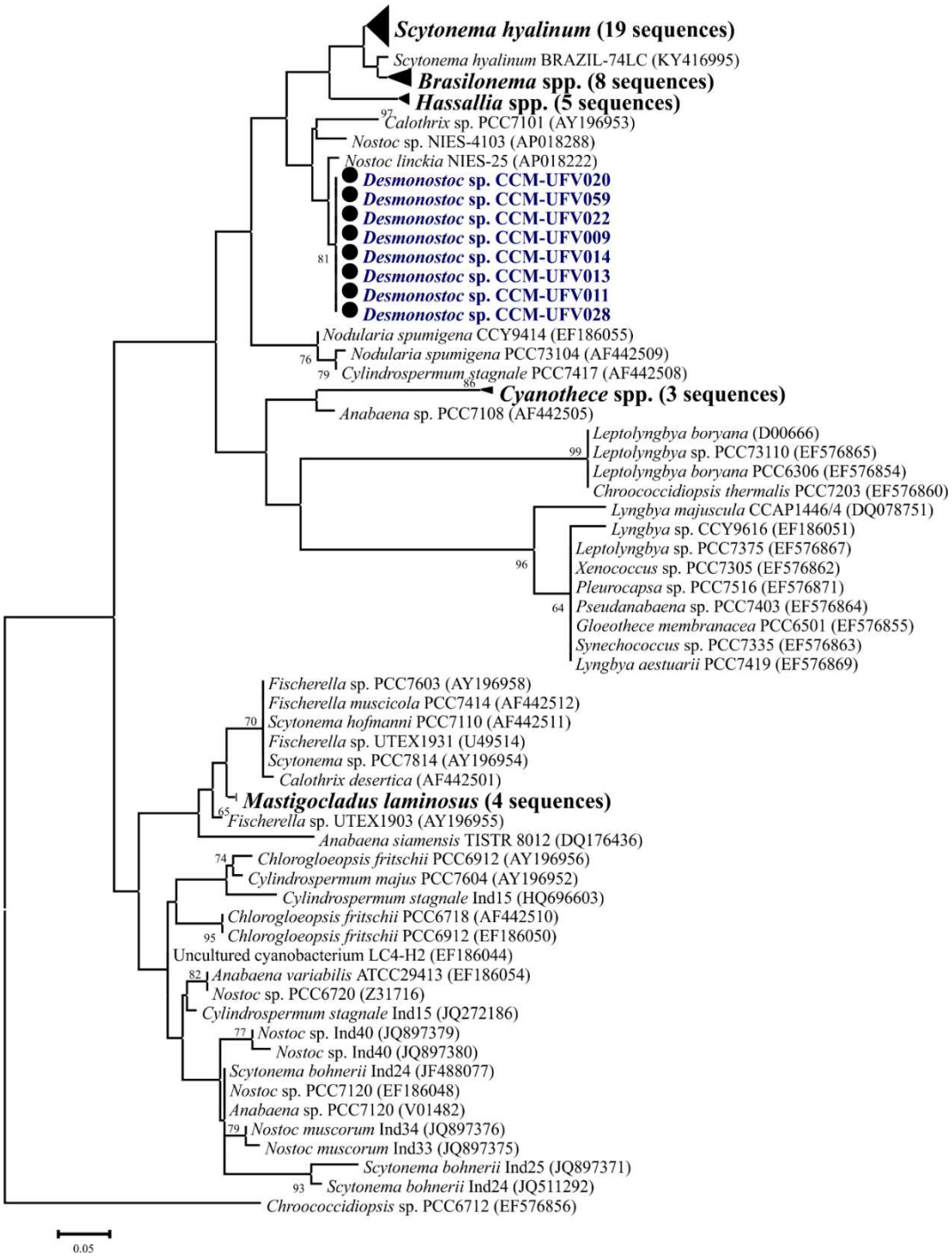

Figure 2. Maximum Likelihood (ML) phylogenetic reconstruction based on partial *nif*D gene sequence. The studied strains are shown in blue-bold with a black circle. A bootstrap test involving 1,000 resamplings was performed and bootstrap values >50 % are given in front of the relevant nodes.

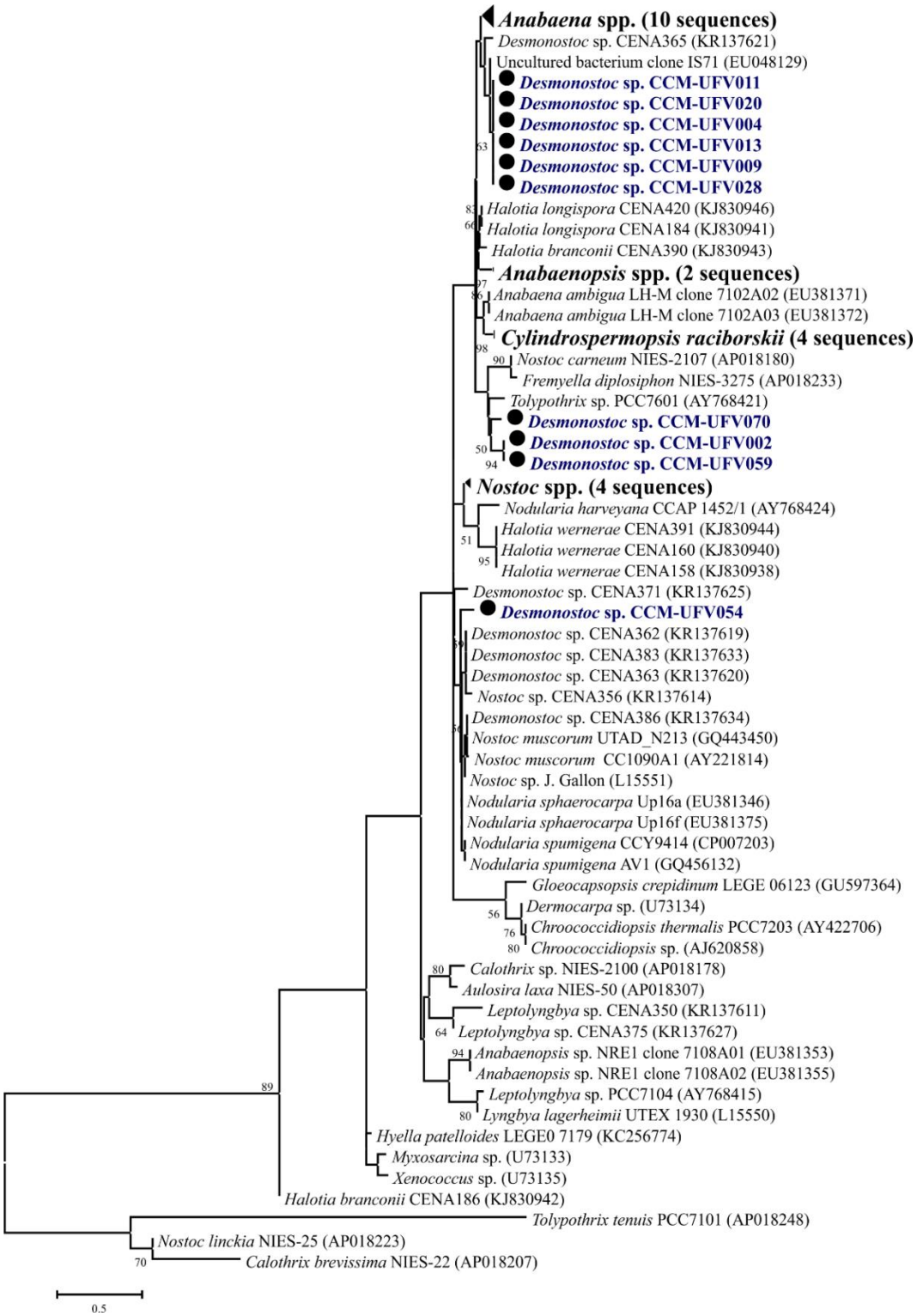

Figure 3. Maximum Likelihood (ML) phylogenetic reconstruction based on partial *nif*H gene sequence. The studied strains are shown in blue-bold with a black circle. A bootstrap test involving 1,000 resamplings was performed and bootstrap values >50 % are given in front of the relevant nodes.

3.3 Morphological characterization

The diversity of morphological types comprised by the studied *Desmonostoc* strains are presented in the Figures 4 and 5. The microscopic aspect of the colonies, formed by a set of parallel trichomes, which has been described as typical for members of the genus *Desmonostoc* (de Alvarenga et al., 2018; Hrouzek et al., 2013) can be observed (Figures 4E, G, J, K, N, Q, R and V). However, this parallel pattern is not observed for the strains CCM-UFV018 and CCM-UFV054, for which the trichomes are homogeneously spread, without a clear organization (Figures 4X and 4Y). As previously reported (de Alvarenga et al. (2018); Hrouzek et al. (2013)), both intercalary and terminal heterocytes werw always presented in the vegetative trichomes. Hormogonia were also observed, mainly in middle-log phase; while akinetes are more frequent at mid-late-stationary phases. Considering the heterocytes, the terminal ones are differentiated during the early stages of trichome development (early-log), being the intercalary heterocytes formed after.

The morphological divergences found for trichome organization are in agreement with the division found in the 16S-based phylogenetic reconstruction, in which sub-clusters A and B were observed. The strains CCM-UFV018 and CCM-UFV054, that display a diffluent trichome organization, were placed in sub-cluster B, while the strains harbored in sub-cluster A present, in general, the typical parallel organization. Interestingly, the morphological traits and morphometric values (Table 2) of the strains placed in the sub-cluster A are similar to those described before (Hrouzek et al. 2013; de Alvarenga et al. 2018). On the other hand, for the strains harbored in the sub-cluster B, we observed divergence in the sizes of vegetative cells, akinetes and heterocytes for the strains CCM-UFV018, CCM-UFV054, CCM-UFV069 and CCM-UFV070. The cellular sizes found for *D. magnisporum* and *D. punense* (Saraf et al., 2018), which are related to CCM-UFV018 and CCM-UFV054 considering the 16S rRNA phylogeny (Figure 1), are substantially shorter than those of our strains, providing a morphological trait that clearly differ our strains from previously described species. In addition, *D. magnisporum* contains akinetes with higher cell length and width, pattern also

observed for the strain CCM-UFV070, a morphological trait that apparently has a correlation with the phylogenetic position of these strains (Figure 1).

Molecular and morphological results suggest therefore that the strains CCM-UFV018 and CCM-UFV054, which presented singular phylogenetic position (Figure 1) and higher cell length (9.63/9.55 µm) and width (9.37/8.16 µm) as well as different growth pattern (Figure 5), must be classified as novel *Desmonostoc* species. It is important to mention that according to Hrouzek et al. (2013) up to that moment, morphological characterization was not an appropriated approach leading to a clear separation of specific units into *Desmonostoc*. These authors also emphasized that morphological traits were not useful in supporting the phylogenetic separation of the clusters D1 and D2. However, as demonstrated here and mainly considering the strains CCM-UFV018 and CCM-UFV054, morphological traits and growth patterns seems to be rather informative for taxa delimitation. Accordingly, it seems reasonable to suggest that other traits, such as physiological ones, can be source of more diacritical elements for a better taxonomic resolution. This fact aside, stable traits must be found, since the morphological diversity found for cyanobacterial strains is usually followed by a great phenotypic plasticity, varying depending on the growth and environment conditions (Berrendero et al., 2011; Lyra et al., 2001; Mateo et al., 2011; Stomp et al., 2008). We posit, therefore, that other characters, like molecular, physiological and metabolic traits as well life cycle, must be used as an important aspects in the characterization and systematic of cyanobacteria (Berrendero et al., 2011; Genuário et al., 2017, 2015; Mateo et al., 2011; Rosmarie Rippka et al., 1979).

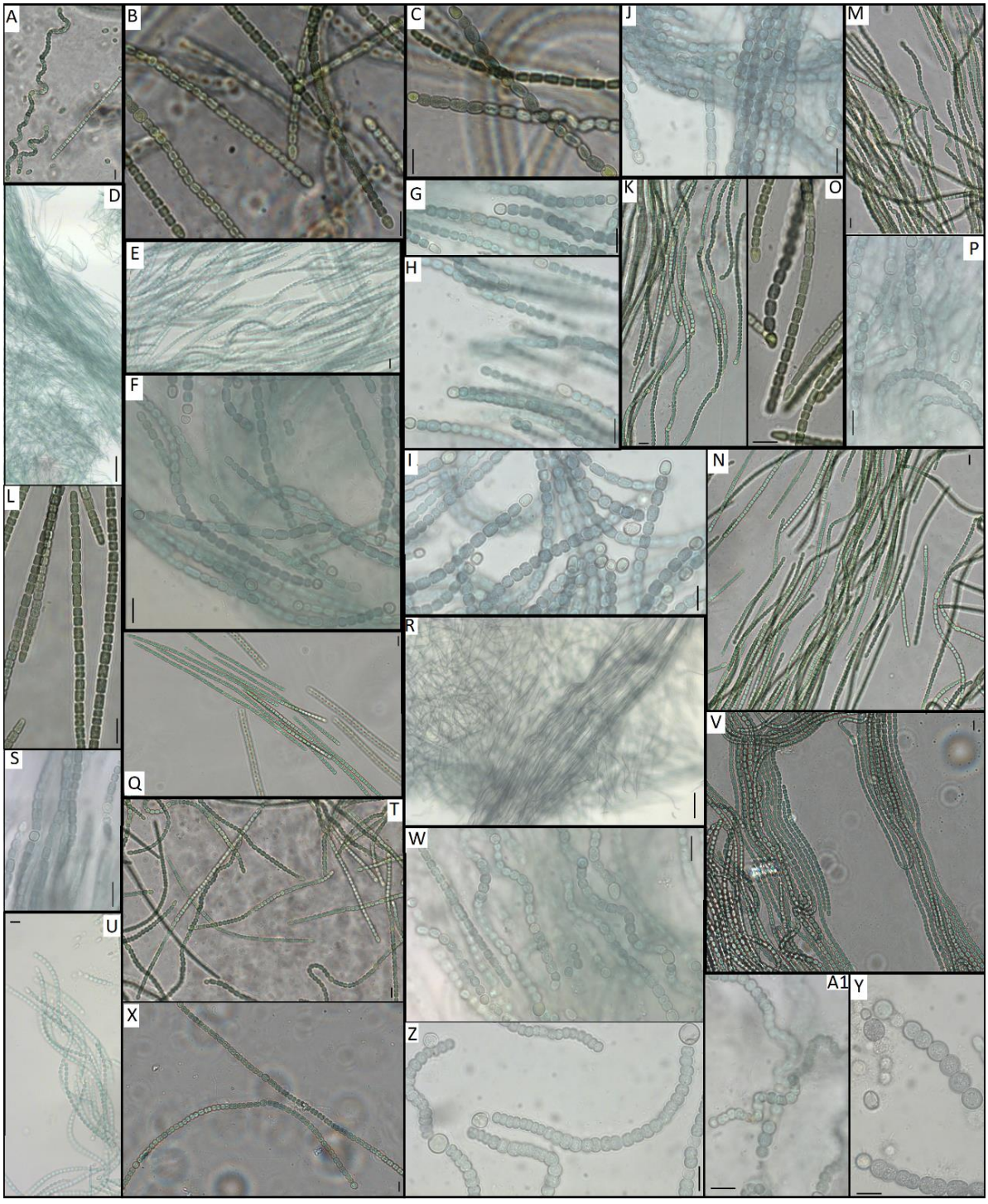

Figure 4. Light photomicrographs from the *Desmonostoc* strains evaluated in this study. A, B, C: CCM-UFV002; D*, E, F: CCM-UFV003; G, H: CCM-UFV004; I, J: CCM-UFV005; K, L: CCM-UFV009; M: CCM-UFV011; N, O: CCM-UFV013; P: CCM-UFV014; Q: CCM-UFV020; R*, S: CCM-UFV022; T: CCM-UFV028; U: CCM-UFV029; V: CCM-UFV031; W: CCM-UFV059; X: CCM-UFV018; ,Y: CCM-UFV054; Z: CCM-UFV070; A1: CCM-UFV069. Scale Bar = 10 µm. *Scale Bar = 100 µm.

Table 2. Morphometric characteristics of the strains used in this study.

Strain	Vegetative cell		Heterocyte		Akinete	
	Length mean (range)	Width mean (range)	Length mean (range)	Width mean (range)	Length mean (range)	Width mean (range)
CCM-UFV002	5.85 (4.42-7.53)	4.91 (3.96-6.07)	8.71 (7.34-9.84)	5.92 (4.56-7.12)	7.54 (5.80-9.43)	5.96 (4.92-6.88)
CCM-UFV003	6.15 (4.68-7.58)	5.33 (4.32-6.18)	6.03 (4.92-8.64)	5.49 (4.75-6.02)	8.55 (7.22-9.38)	5.69 (4.67-6.25)
CCM-UFV004	6.19 (5.38-7.16)	5.80 (5.00-6.67)	7.22 (5.47-9.13)	6.09 (5.19-7.22)	9.10 (8.69-10.1)	6.26 (5.43-7.25)
CCM-UFV005	6.26 (5.14-7.16)	5.94 (3.97-7.28)	6.85 (4.84-9.30)	5.84 (4.80-6.85)	9.19 (6.24-10.9)	6.13 (4.75-7.26)
CCM-UFV009	5.41 (4.20-6.44)	4.96 (4.28-5.98)	7.21 (5.15-8.95)	6.05 (5.00-7.07)	9.19 (7.35-10.4)	5.92 (5.17-6.72)
CCM-UFV011	6.86 (4.50-8.05)	5.62 (4.67-6.37)	7.93 (6.94-9.70)	5.50 (4.60-6.28)	8.79 (7.49-11.6)	6.29 (5.64-7.09)
CCM-UFV012	6,36 (4.86-8.26)	5.85 (5.18-6.59)	7.19 (6.06-7.88)	5.54 (4.93-6.95)	9.10 (6.78-10.1)	7.15 (5.44-9.17)
CCM-UFV013	6.62 (5.51-8.88)	5.80 (5.11-6.74)	8.63 (6.35-10.6)	6.31 (5.28-7.14)	9.72 (6.64-11.1)	6.71 (6.05-7.56)
CCM-UFV014	6.25 (4.47-7.42)	5.69 (5.76-6.86)	7.28 (5.00-9.44)	5.91 (3.76-8.39)	9.37 (7.49-12.0)	6.02 (5.11-7.28)
CCM-UFV020	5.57 (4.53-6.93)	5.21 (4.00-6.61)	7.48 (5.03-9.22)	5.77 (4.55-6.80)	8.35 (6.54-9.90)	5.63 (4.68-6.48)
CCM-UFV022	5.82 (4.55-8.26)	4.68 (3.84-5.40)	7.33 (5.81-8.84)	5.23 (4.11-6.97)	8.14 (6.87-10.1)	5.22 (4.34-6.85)
CCM-UFV028	7.03 (5.34-8.69)	5.48 (4.72-6.14)	7.25 (5.25-8.54)	6.30 (4.23-8.34)	9.09 (7.94-11.0)	6.52 (5.60-7.62)
CCM-UFV029	5.62 (4.39-7.43)	5.51 (4.20-6.53)	7.90 (4.39-10.3)	5.35 (4.36-6.37)	8.20 (6.84-8.91)	6.53 (5.76-7.69)
CCM-UFV031	6.59 (5.25-8.94)	5.06 (4.02-6.21)	7.97 (6.44-9.97)	6.04 (4.62-7.30)	9.15 (8.55-10.6)	5.38 (4.71-6.07)
CCM-UFV059	5.45 (4.25-6.61)	5.11 (4.23-5.92)	6.06 (3.89-9.26)	5.05 (3.68-5.84)	8.42 (6.08-10.6)	6.12 (4.64-7.26)
CCM-UFV018	**9.63 (8.66-11.9)***	**9.55 (8.49-10.4)***	**10.9(7.05-12.0)***	**9.38 (7.04-10.4)***	10.3 (8,87-14,5)	**8.11 (6.52-10,1)***
CCM-UFV054	**9.37 (6.16-12.6)***	**8.16 (6.75-9.80)***	**9.94 (6.77-13.7)***	**9.06 (8.36-10.6)***	**12.8 (11.4-13.3)***	**9.51 (9.04-13.5)***
CCM-UFV069	5.98 (4.91-6.98)	5.15 (3.84-6.01)	6.33 (4.67-7.67)	5.78 (4.83-6.68)	7.21 (5.76-9.07)	**7.46 (6.46-8.17)***
CCM-UFV070	6.40 (5.04-7.32)	**6.87 (6.19-7.44)***	8.31 (7.49-9.57)	**8.08 (7.36-9.10)***	**11.08(8.71-15.3)***	**9.49 (8.22-11.7)***
***D. muscorum* II**	4.70 (2.80–6.80)	4.90 (4.00-5.90)	7.40 (5.30-10.2)	5.80 (4.40-7.20)	7.00 (4.5–9.4)	4.90 (3.4–6.3)
***D. muscorum* NIVA–CYA 817**	5.50 (3.60–7.70)	5.70 (4.00-6.80)	8.60 (6.20-11.1)	6.50 (5.00-8.30)	8.60 (5.4–12.5)	5.60 (3.8–8.0)
***D. muscorum* 1/87**	4.70 (3.30–7.90)	3.40 (2.70-4.50)	5.60 (4.00-7.00)	4.50 (3.50-5.10)	6.40 (4.5–8.1)	5.00 (3.9–6.3)
***D. muscorum* NIVA–CYA 818**	5.0 (3.20–7.90)	4.90 (3.80-6.30)	8.10 (5.50-11.3)	6.40 (4.50-8.70)	7.60 (5.5–8.8)	4.50 (3.7–5.1)
***D. muscorum* De**	4.0 (2.30–6.30)	4.40 (3.40-5.40)	7.80 (6.80-8.70)	6.70 (5.80-7.40)	7.00 (5.9–8.0)	5.30 (3.6–6.9)
***Desmonostoc* sp. PCC8306**	4.6 (2.80–7.50)	4.40 (3.20-5.40)	5.70 (3.80-9.20)	4.70 (3.60-5.90)	9.70 (8.5–9.9)	5.60 (5.0–6.1)
***Desmonostoc* sp. TO1SO1**	5.0 (2.90–7.60)	3.40 (2.70-4.10)	4.50 (3.40-7.10)	3.60 (2.90-4.70)	8.20 (7.1–8.5)	4.60 (4.4–4.7)

All values are show in µm. The measures followed by an asterisk (*) and highlighted in bold are significantly different according to Tukey test (5%). The strains marked as green and orange belong to sub-clusters A and B, respectively. The remaining strains were described before (Hrouzek et al., 2013).

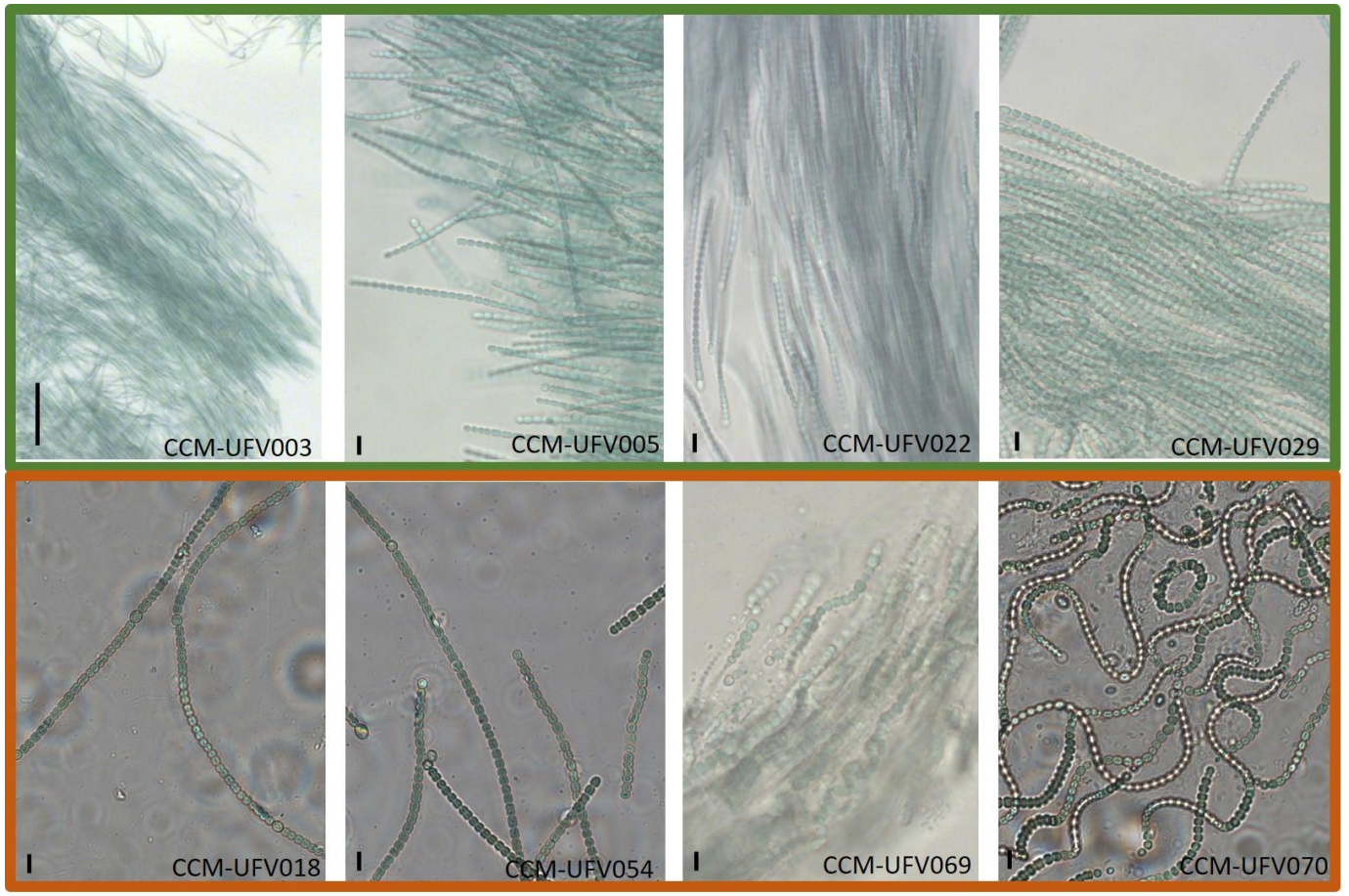

Figure 5. Light photomicrographs from selected *Desmonostoc* strains from Cluster A (CCM-UFV003, CCM-UFV005, CCM-UFV022 and CCM-UFV029) and Cluster B (CCM-UFV018, CCM-UFV054, CCM-UFV069 and CCM-UFV070), according to Figure 1. Scale Bar = 10 µm. For CCM-UFV003, Scale bar = 100 µm.

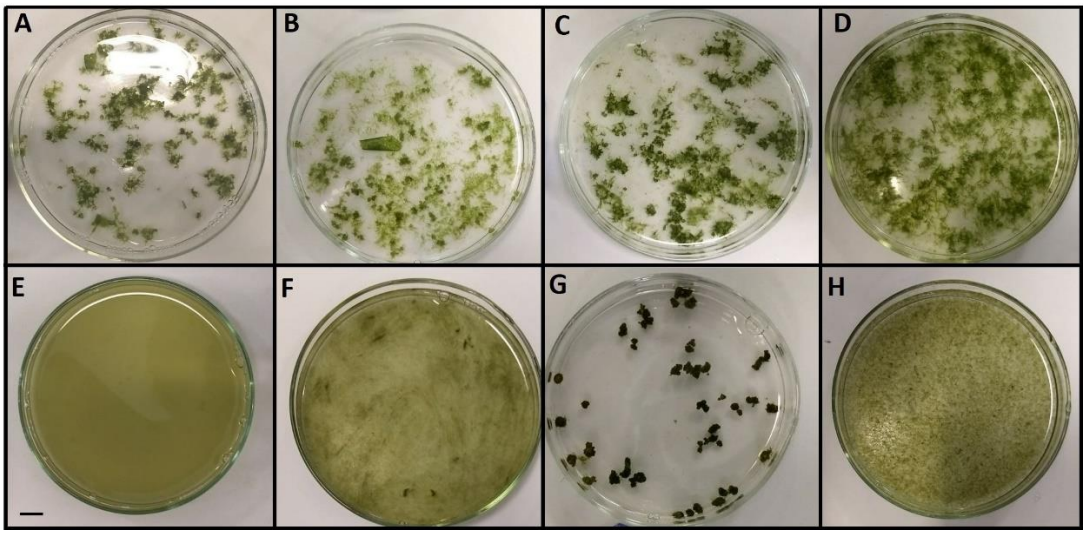

Figure 6. Images showing the macroscopic aspect of *Desmonostoc* strains selected for metabolic analysis. All strains were grown in liquid BG-11_0 culture medium. The cultures were grown for 10 days and then dropped into Petri dishes. A: CCM-UFV003; B: CCM-UFV012; C: CCM-UFV020; D: CCM-UFV059; E: CCM-UFV018; F: CCM-UFV054; G: CCM-UFV069; H: CCM-UFV070. Scale bar = 1 cm.

3.4 Photosynthetic parameters

Aiming to find the most appropriate light intensity for cyanobacterial growth, we also investigated the photosynthetic light response of the *Desmonostoc* strains. The *Desmonostoc* strains analyzed here displayed great differences considering both saturation (I_s) and compensation (I_c) points, which ranged from 40-80 and 5-25 µmol·photons m^{-2}·s^{-1}, respectively (Table 3). It is important to mention that this diversity in terms of physiological parameters was not linked to their morphology or phylogenetic placement (sub-cluster A and B – Figure 1). The higher I_s (80 µmol·photons m^{-2}·s^{-1}) was found for the strains CCM-UFV059 and CCM-UFV011. Considering their sampling sites, it was not possible to build any relation between their isolation sources and their I_s.

Table 3. Variation in saturation irradiance (*Is*) and compensation irradiance (*Ic*) obtained for all *Desmonostoc* strains available at CCM-UFV.

Strain	*Is* (µmol·phtotons $m^{-2}·s^{-1}$)	*Ic* (µmol·photons $m^{-2}·s^{-1}$)
CCM-UFV002	40	15
CCM-UFV003*	50	13
CCM-UFV004	60	11
CCM-UFV005	40	15
CCM-UFV009	50	17
CCM-UFV011	80	12
CCM-UFV012*	50	25
CCM-UFV013	40	11
CCM-UFV014	60	15
CCM-UFV020*	60	15
CCM-UFV022	60	16
CCM-UFV028	70	17
CCM-UFV029	50	5
CCM-UFV031	70	15
CCM-UFV059*	80	16
CCM-UFV018*	70	16
CCM-UFV054*	70	15
CCM-UFV069*	70	15
CCM-UFV070*	50	11

The strains marked as green and orange belong to sub-cluster A and B respectively. The strains marked with asterisk (*) and highlighted in bold were selected for metabolic and physiological analysis. Values are presented as means (n = 3).

Despite of the range in I_s and I_c, a deep comparison with data from literature was not possible, since most of the studies dealing with physiological characterization of *Desmonostoc* strains did not focus on this trait. Interestingly, in a previous study conducted with a subset of CCM-UFV cyanobacterial strains (Esteves-Ferreira et al., 2019 – unpublished), similar values for nostocacean strains were found, which ranged from 8-25 and 56-92 µmol·photons $m^{-2}·s^{-1}$, for I_c and I_s, respectively. Specifically, for the strain CCM-UFV020, which was previously named as *Nostoc* sp., the I_c and I_s values were, respectively, 23 and 80 µmol·photons $m^{-2}·s^{-1}$ (Esteves-Ferreira et al., 2019), while here we found lower values, 15 and 60 µmol·photons $m^{-2}·s^{-1}$ for I_c and I_s, respectively. These minor differences can be explained by the light intensity used for pre-inoculum production (50 µmol·photons $m^{-2}·s^{-1}$) in our and 60 µmol· photons $m^{-2}·s^{-1}$, applied by Esteves-Ferreira et al. (2019). More important, this range of I_s is typically observed for “shading” strains (Whitton,

2000), data also corroborated by the I_c which, ranged from 5 to 25 µmol·photons $m^{-2}·s^{-1}$. Additionally, the genetic background and the conditions of pre-growth probably had more influence on this results than the original sampling sites (Komárek and Anagnostidis, 1989; Rosmarie Rippka et al., 1979)

3.5 Growth curves and kinetics parameters

Growth curves and kinetics parameters as well as biomass production data were obtained for eight strains, which were selected considering their morphological dissimilarities (Figure 4) and phylogenetical placement (Figure 1). The strains CCM-UFV003, CCM-UFV012, CCM-UFV020 and CCM-UFV059 belong to the sub-cluster A (Figure 1) and display a typical parallel trichome organization (Figure 5), while the strains CCM-UFV018, CCM-UFV054, CCM-UFV069 and CCM-UFV070 are harbored into sub-cluster B (Figure 1), showing a non-typical macroscopic growing pattern (Figure 6).

Overall, lag phases were absent for all eight strains, while log phases varied from 5 to 7 days, followed by a linear (slow downing) phase. The stationary phase was reached after 8-10 cultivation-days (Figure 7 and 8). However, it is important to highlight that the pattern found for the selected *Desmonostoc* strains are coherent with the sub-clusters A and B observed in the phylogenetic reconstruction (Figure 1). The strains CCM-UFV012, CCM-UFV020 and CCM-UFV059, which belong to sub-cluster A exhibited similar growth curves, showing one or two non-growing days (Figure 7), respectively at days 4-5, 5-7 and 5-6. Accordingly, as shown in Figure 5, these strains form rigid colonies when growing in liquid medium, fact that can lead to stressful light conditions in the inner part of the colonies. This stressful condition can, in turn, lead to intense hormogonia differentiation, which was corroborated by microscopic observation (data not shown).

The hormogonia filaments have been described as motile trichomes (gliding motility or gas vesicle-containing trichomes) involved in reproduction and dispersion of the cyanobacterial strains able in its differentiation (Flores and Herrero, 2010; Marsac, 1994). More importantly, these motile trichomes shown a pattern of intense cell division without biomass production, causing this observed “pause” on the growth, when its differentiation is massive. This

lack on biomass production is explained by the absence of heterocytes and PSII (Papaefthimiou et al., 2008; Rosmarie Rippka et al., 1979; Somero, 1992), impairing the adequate biological nitrogen fixation and photosynthesis, respectively. This high aggregated pattern was also observed for the strain CCM-UFV069 (Figure 5G), despite of its phylogenetic placement in the sub-cluster B (Figure 1). This pattern can justify, at least partially, a non-growing period (between the days 6-9) observed in the growth curve of this strain (Figure 8).

A different pattern was observed for the strains CCM-UFV018, CCM-UFV054 and CCM-UFV070, which belong to sub-cluster B (Figure 1) and display a diffluent macroscopic pattern (Figure 6). This gelatinous aspect is consequence of the high amount of exopolysaccharides (EPS) produced by these strains, contributing to a less aggregate colony pattern. Thus, it seems plausible to hypothesize that the incident light is more homogeneously distributed than in the case of the strains harbored in the sub-cluster A. Accordingly, the hormogonia differentiation is less frequent or even absent in such strains.

The pH values found along the growth curves also present a difference considering the strains belonging to sub-cluster A and B. The strains from sub-cluster B show more variable pH values, compared to those from cluster A. It is possible to observe that the pH values increased at the beginning of growth, and at the end, for strains belonging to sub-cluster B, possibly related with the input of nutrients, mainly inorganic carbon from de surrounding medium, during growth. This data might be related with the Carbon concentration mechanism (CCM), since the input of carbon can alter the pH of medium (Mangan et al., 2016).

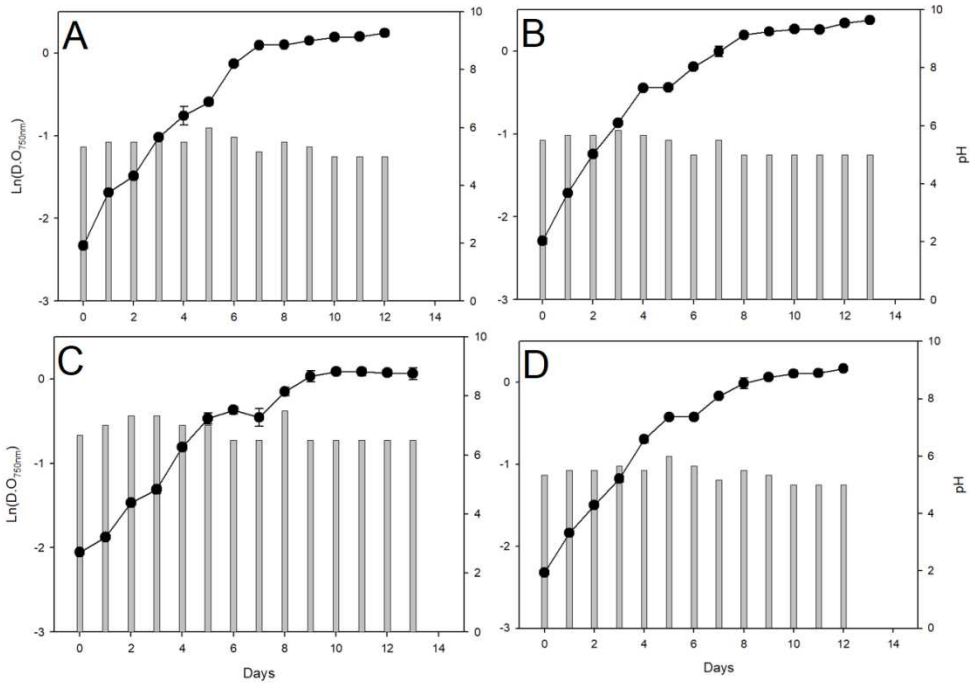

Figure 7. Growth curves of *Desmonostoc* spp. from sub-cluster A, grown in BG-11_0 medium. A: CCM-UFV002, B: CCM-UFV012, C: CCM-UFV020, D: CCM-UFV059. In Y Axis, Ln(DO_{750nm}) (left), and pH (right side). In X axis, time in days.

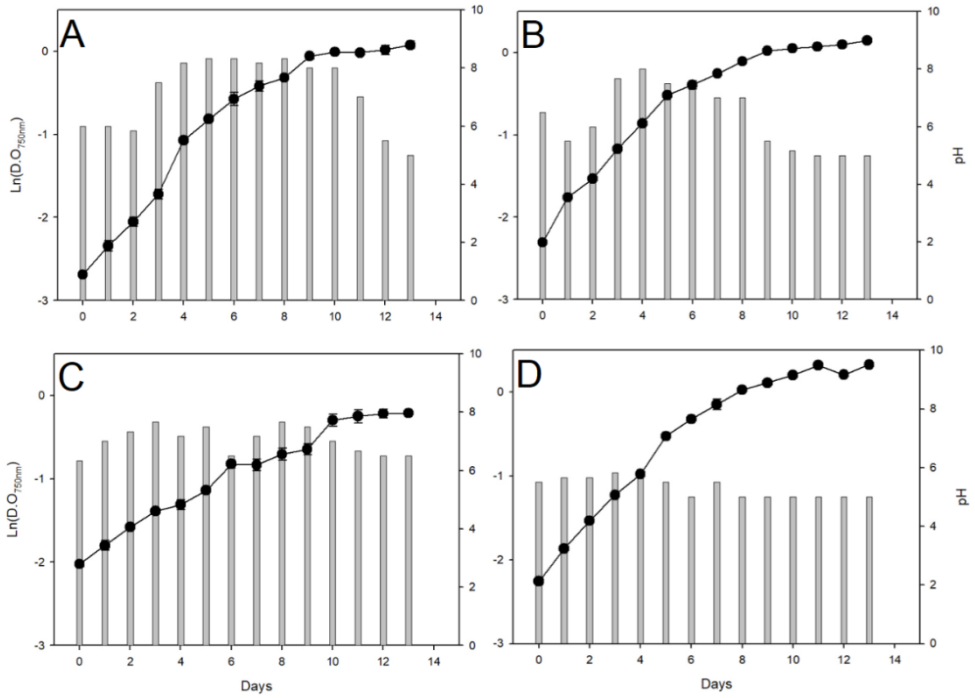

Figure 8. Growth curves of *Desmonostoc* spp. from sub-cluster B, grown in BG-11_0 medium. A: CCM-UFV018, B: CCM-UFV054, C: CCM-UFV069, D: CCM-UFV070. In Y Axis, Ln(DO_{750nm}) (left), and pH (right side). In X axis, time in days.

For the $\mu_{(max)}$, that corresponds to the maximum growth rate at logarithmic phase, the strains CCM-UFV069 and CCM-UFV054 displayed the lower values, while the strains CCM-UFV012 and CCM-UFV018 the higher ones (Indicar a Tabela). The strain CCM-UFV012, with the higher $\mu_{(max)}$, also presented the higher biomass production (1.694 $mg \cdot mL^{-1}$), after 13 growing days. In the same way, the strain CCM-UFV069, which displayed the lower $\mu_{(max)}$, also presented low biomass production (0.8 $mg \cdot mL^{-1}$) (Indicar a Tabela). However, for the other strains it was not possible to find a clear relation between $\mu_{(max)}$ and biomass production, even considering the phylogenetic relatedness of members of sub-clusters A and B. The average values observed for biomass increment and production are similar to those found for *Nostoc* and *Anabaena* strains (Rosales-Loaiza et al., 2017). The exceptions are the strains CCM-UFV069 and, in some extent, the strain CCM-UFV054, which showed a lower biomass increments/production as well as $\mu_{(max)}$.

Table 4. Natural variation in growth, kinetics parameters and biomass production among the *Desmonostoc* strains used for growth and metabolic analysis.

Strains (CCM-UFV)	$\mu_{(max)}$	DT*(hours)	Biomass increment ($mg \cdot mL^{-1} \cdot d^{-1}$)	Biomass ($mg \cdot mL^{-1}$)
CCM-UFV003	0.380 **bcd**	43,72	0.1017	1.323
CCM-UFV012	0.453 **a**	36,65	0.1303	1.694
CCM-UFV020	0.347 **cde**	41,24	0.0918	1.194
CCM-UFV059	0.391 **bc**	47,92	0.0960	1.248
CCM-UFV018	0.403 **b**	52,60	0.0985	1.280
CCM-UFV054	0.316 **e**	42,49	0.0878	1.141
CCM-UFV069	0.180 **f**	91,30	0.0616	0.800
CCM-UFV070	0.332 **de**	50,03	0.0923	1.200

*DT = Doubling Time. All measurements were conducted in triplicates. The biomass values were obtained after 12-13 days of growth (Figure 7 and 8). The strains marked as green and orange belong to sub-clusters A and B, respectively. Different lower case letters across columns indicate mean values that are significantly different according to Tukey test.

The difference in growth and biomass accumulation between the strains CCM-UFV069 and CCM-UFV070 is rather interesting since they were isolated from the same environment (Obuekwe et al., 2019). Both strains were isolated from Arsenic-contaminated area, being able to growth under different Arsenic concentrations (data not shown). Accordingly, these strains can be explored in bioremediation processes, and the growth parameters obtained here can

aid into the selection of appropriated strains for biotechnological applications that result in viable bioremediation solutions

3.6 Molecular screening results

The molecular screening for genes involved in the biosynthesis of cyanotoxins (microcystin and saxitoxin) as well as protease inhibitor (microviridin) did not produce any positive reaction, indicating that all CCM-UFV *Desmonostoc* strains do not carry the genetic potential to produce these compounds. It should be mentioned that, to date, there is no register of *Desmonostoc* strains capable of producing the screened compounds. This fact apart it is important to mention that brazilian *Desmonostoc* strains isolated from Atlantic coastal forest have been reported as anabaenopeptins and cyanopeptolins-producers, which are cyanopeptides with protease inhibitor activities (Sanz et al., 2015).

3.7 Metabolic characterization

3.7.1 Chlorophyll *a*

For all metabolic analysis, the samples were collect in the middle of light phase in the end of the growth curves. The strains CCM-UFV003, CCM-UFV012, CCM-UFV020 and CCM-UFV054 showed the highest chlorophyll *a* contents, followed by the strains CCM-UFV018, CCM-UFV070, CCM-UFV059 and CCM-UFV069, being the lower content found for the last strain (Figure 9A). These values are similar to those already reported for nostocacean strains (Bhunia et al., 1991; Jaiswal et al., 2018). For the sub-cluster A, the lower chlorophyll *a* content found for the strain CCM-UFV059 can be explained by its higher I_s in comparison with the other strains from this sub-cluster. To avoid photo oxidative damages, the chlorophyll content seems to be reduced with more light, which has been observed for *Spirulina* (Kumar et al., 2011). Interestingly, the I_s of the strains CCM-UFV003, CCM-UFV12 and CCM-UFV20 are similar (50-60 $\mu moles \cdot m^{-2} \cdot s^{-1}$; Table 3), leading to similar chlorophyll *a* contents. This show a possible association between the

chlorophyll *a* levels and the light intensity of growth, since the strains growth under the same irradiance as those found for their I_s.

The strains belonging to the sub-cluster B (hatched bars – Figure 9A) had a greater variation in chlorophyll *a* contents, ranging from 4 µg·mg^{-1} DW to 8 µg·mg^{-1} DW, with CCM-UFV069 possessing the lower levels of chlorophyll *a*. The higher levels of chlorophyll *a* found for the strains CCM-UFV018 and CCM-UFV054 and the high I_s can explain partially why this strains can sustain an constant growth, providing carbon skeletons, which in turn may be used for amino acids biosynthesis and production of exopolysaccharides. Nevertheless, our data provide only circumstantial evidence for this assumption and further studies are clearly required to enhance our understanding of carbon and nitrogen fixation within this strains.

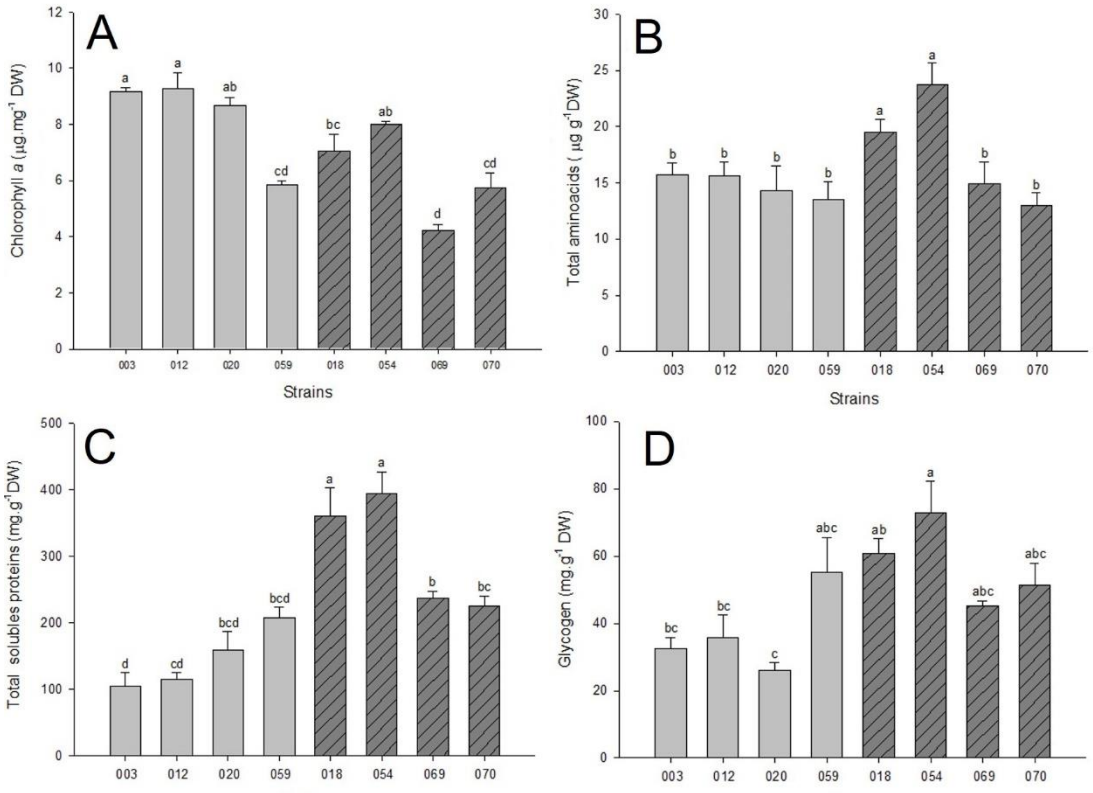

Figure 9. Metabolites concentration in the studied *Desmonostoc* strains. (A) Chlorophyll *a*; (B) Total amino acids; (C) Total protein; (D) Glycogen. Values are presented as means ± standard deviation (n = 4). The clean and hatched bars are in reference to the strains from sub-clusters A and B, respectively. Means followed by the same letter do not differ by 5% of probability (Tukey's test).

3.7.2 Amino acids and total proteins

The total amino acids contents of *Desmonostoc* spp. ranged from 13 µg·mg^{-1} DW for CCM-UFV070 to 23 µg·mg^{-1} DW for CCM-UFV054 (Figure 9B).

Considering the contents of total amino acids and total soluble proteins (Figure 9B and 9C), the strains belonging to sub-cluster A, seems to have a negative correlation between these metabolites, as already expected, since the protein synthesis and degradation are directly linked, if the amino acids synthesis remain constant, at least in plants (Hildebrandt et al., 2015) and also for certain cyanobacterial strains (Esteves-Ferreira et al., 2019). However, for the strains belonging to sub-cluster B it is possible to observe a positive correlation between these metabolites (Figure 9). We hypothesize that “sub-cluster B” strains have either an intense (higher) amino acids synthesis, as consequence of possible high rates of biological nitrogen fixation, or present high concentration of other compounds, which are structurally similar to amino acids (such as mycosporine-like amino acid) (Colabella et al., 2015), contributing to the higher levels of amino acids. It is important to mention that some *Nostoc* and *Anabaena* strains are able to produce mycosporine-like amino acid (Katoch et al., 2016), although these compounds and their biosynthetic pathways were not quantified or screened in our *Desmonostoc* strains. In addition, the lower levels of amino acids coupled to high protein contents found for the “sub-cluster A” strains can be an indicative of high rates of protein synthesis, which are probably able to sustain the higher growth rates observed for these strains (Table 4).

For the total soluble proteins, higher levels were found for the strains CCM-UFV018 and CCM-UFV054, reaching almost 40 % of total cell weight (Figure 9). The protein contents found for our *Desmonostoc* strains are in agreement with previous reports, which demonstrate that cyanobacteria have a protein content varying from 10 % to 60 % based on cell weight (Kumar et al., 2011; Spolaore et al., 2006). The planktonic behavior of the strains CCM-UFV018 and CCM-UFV054 can be an explanation of the high protein content, by the fact that the gas vesicles, used for the buoyance, are basically constituted of great amounts of protein (Walsby and Hayes, 1989). Also, the highly protein content of CCM-UFV018 and 054 make then good candidate to biotechnological and industrial applications.

3.7.3 Phycobiliproteins (PBP)

The values found in our analysis for total phycobiliproteins (PBP) quantification ranged from 17 µg·mg^{-1} DW (CCM-UFV069) to 34 µg·mg^{-1} DW (CCM-UFV018) (Figure 10). Values of 8 to 400 µg.mg of total phycobiliproteins were observed for some terrestrial strains (Manoj Kumar, Jyoti Kulshreshtha, 2011; Sekar and Chandramohan, 2008; Simeunović et al., 2013; Soltani et al., 2006). This indicates that the values found for *Desmonostoc* strains described here are in agreement with those reported before.

The PBP contents apparently have a difference between the cluster A and B. The lowers levels of total PBP were found for the strain CCM-UFV069 (sub-cluster B). The PBP are related with the light harvesting system, and the saturation point and the contends of PBP appear to not have correlation for *Desmonostoc* spp. So in this case, been probably more related with specific genetic traits. For the strains CCCM-UFV018 and CCCM-UFV054, the higher levels of PBP probably have a relation with the total amino acids and protein levels, since PBP serve as a nitrogen storage compound (de Marsac and Houmard, 1988; Simeunović et al., 2013). Accordingly, the high levels of those metabolites may have stimulate the synthesis of PBP, beside the specific traits of those strains. This data corroborates to the separation of these strains, CCM-UFV018 and 054, as distinct lineage.

It is also important to mention that the lower levels of PBP observed for CCM-UFV069 shed light on a singular trait of this strain, that is the presence of higher amounts of allophycocyanin (Ap), compared to phycoerythrin (Pe) and phycocyanin (Pc), which is highly uncommon (Cuellar-Bermudez et al., 2015). In general, Pc has been reported as the most abundant PBP in the majority cyanobacteria (Basheva et al., 2018; Gupta et al., 2018; Kaushal et al., 2017; Khazi et al., 2018; Pagels et al., 2019).

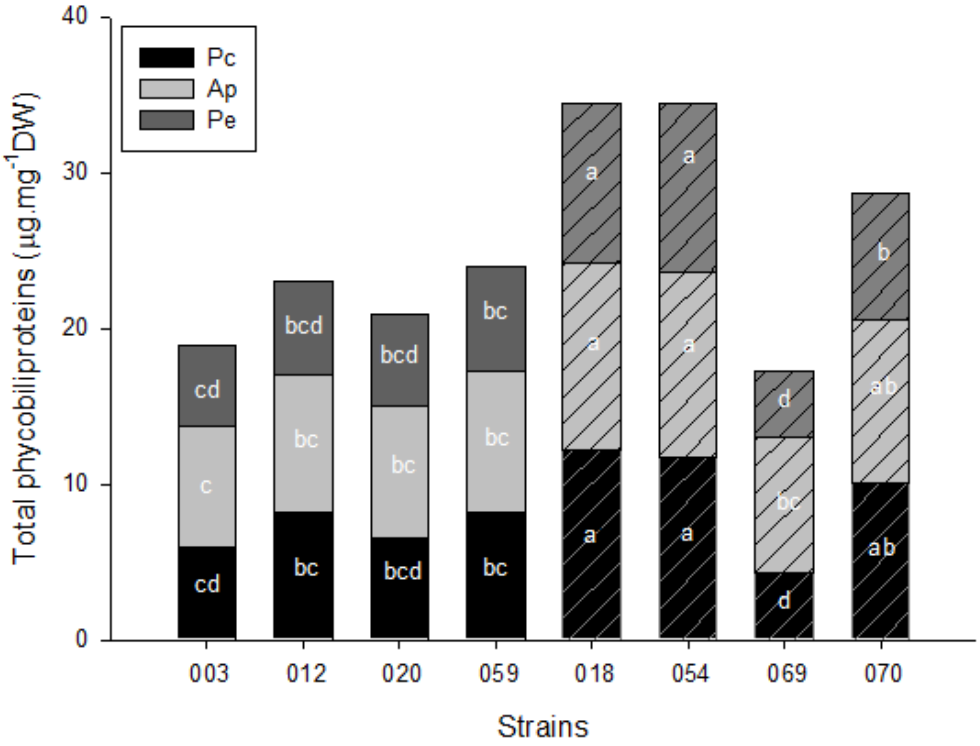

Figure 10. Total Phycobiliproteins content. Pc: Phycocyanin; Ap: Allophycocyanin; Pe: Phycoerythrin. Values are presented as means ± standard deviation (n=3). The clean and hatched bars are in reference to sub-cluster A and B respectively. Means followed by the same letter do not differ by 5% of probability (Tukey's test).

This data brings another physiological difference that corroborate with the hypothesis that these strains, CCM-UFV018/054 and probably CCM-UFV069, should be classified as different species. The higher protein levels observed in these strains is not an indicative that these proteins are functional proteins, since they growth rates are rather low (Figure 8), and the PBP contents are high (Figure 10). Accordingly, part of the total protein is in the PBP (storage and light harvesting) instead of being used as active metabolic proteins. Further studies should be performed to explain this intriguingly metabolic feature.

3.5.3 Glycogen

Glycogen is a carbon storage compound found in cyanobacterial cells, similarly to starch in plants (Herrero and Flores, 2019; Zhang et al., 2018),and also function as a main energy source during the dark period (Knoop et al., 2013). The values found here ranged from 26 mg·g^{-1} DW for the strain CCM-

UFV020 to 72 mg·g^{-1} DW for the strain CCM-UFV054 (Figure 9D). The higher values of glycogen were found for sub-cluster B strains, and also for the strain *D. salinum* CCM-UFV059. The lower value was found in CCM-UFV020 (Figure 9D). The higher values in sub-cluster B strains may have indicate that those strains have a higher requirement of carbon during dark periods, or long-term storage necessities, but a quantification of glycogen during the dark period is necessary to confirm this hypothesis. Another hypothesis that can explain the higher levels of glycogen is the homeostasis of C/N ratio (Herrero and Flores, 2019; Muro-Pastor and Florencio, 2003; Zhang et al., 2018). The strains belonging to sub-cluster B had higher levels of proteins and amino acids, indicating high BNF rates. In an opposite way, the rapid growth of the strain CCM-UFV020, which belong to sub-cluster A, and the lower glycogen contends may be a indicative of the carbon assimilation efficient of this strain, suggesting that the carbon assimilated is incorporated in biomass, instead of building storage for stress or dark periods.

Considering that the sampling points for the metabolic analyses were in the early-to-mid-stationary phase for all strains, and that these strais were grown in their “optimal condition” (light intensity close to the saturation point and BG-11$_0$ medium), it should be possible that massive akinetes differentiation has took place, changing the expected levels of some metabolites (Mateo et al., 2011). However, the levels of PBP and of other metabolites as well as microscopic inspection confirmed the abundance of vegetative cells. Accordingly, the observed levels of each metabolite, pigment and storage compound are in fact consequence of the natural variation among the selected *Desmonostoc* strains. Taken together, these traits can be surely used as a new branch for a more robust “polyphasic characterization”.

3.6 PCA

To explore in more detail the overall variation among the *Desmonostoc* strains, some of the data obtained was analyzed using PCA. The PCA was constructed with the most significant data obtained after a factor analysis (cell measures, phycobiliproteins, glycogen, chlorophyll and $\mu_{(max)}$). The clustering was realized by both partitional (K-means, k = 4) and agglomerative (Ward’s

method) methods, and no differences between those analysis was obtained. The first two components of PCA covered over 87.95 % of the total variance, with 69.69 % and 18.26 % for component 1 (PC1; x-axis) and 2 (PC2; y-axis), respectively (Figure 11). Notably, this analysis corroborates with most of results described in this work, indicating that CCM-UFV018 and 054 are indeed distinct strains. In addition, a clear separation of the strains CCM-UFV070 and CCM-UFV069 were observed, putting these strains as distinct types, despite their same sampling site (Obuekwe et al., 2019). The strains belonging to sub-cluster A (CCM-UFV003, CCM-UFV012, CCM-UFV059 and CCM-UFV020) were spread into one large group. The main metabolic traits explaining this separation between groups along PC1 are alophycocyanin and phycoerithrin, and for PC2 are $\mu_{(max)}$ and chlorophyll (Table 5).

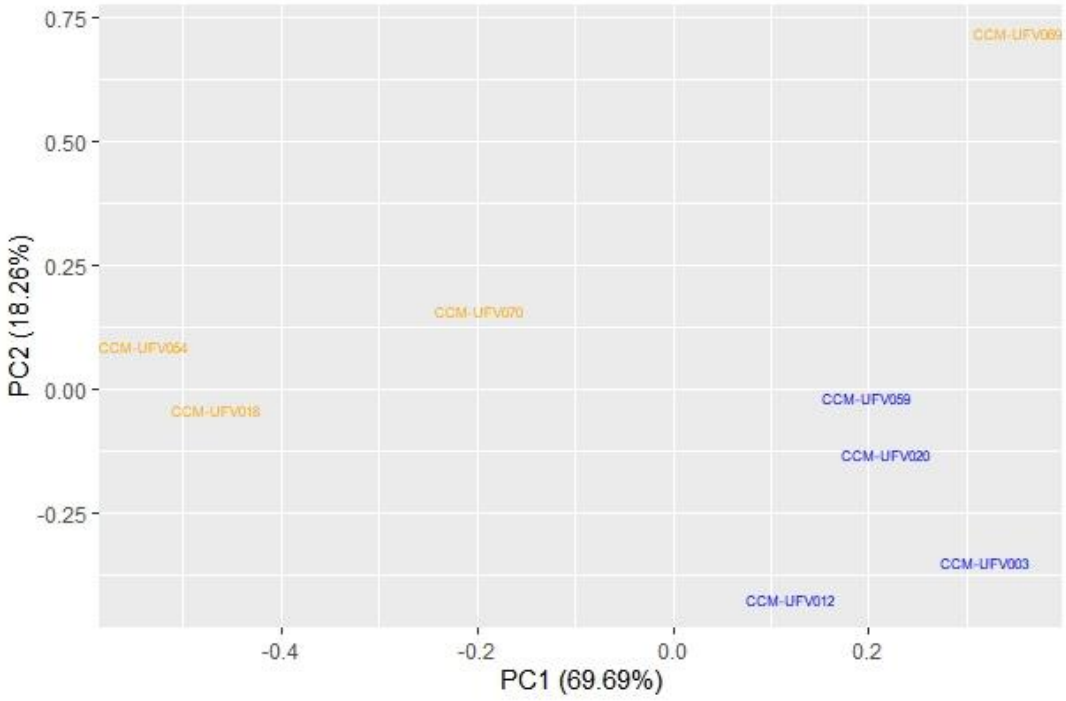

Figure 11. Principal component analysis (PCA) of the growth, morphological and metabolic parameters obtained for the eight *Desmonostoc* strains. PCA was performed using the following variables: morphological (vegetative cell, heterocytes and akinetes length and width), metabolic (phycobiliproteins, glycogen and chlorophyll contentes) and growth ($\mu_{(max)}$). *Desmonostoc* strains from the sub-cluster A (blue labels); *Desmonostoc* strains from the sub-cluster B (orange labels).

Table 5. PCA variables with the contribution value for each component.

Variable	PC1	PC2
Alophycocyanin	-0.33526669	0.128893751
Phycoerithrin	-0.33381462	-0.100007952
Vegetative.Width	-0.33312653	-0.007864310

Heterocyte.Width	-0.32842991	0.122454844
Heterocyte.Length	-0.31667194	-0.011609044
Akinetes.Length	-0.31636023	-0.141029108
Phycocianin	-0.31446929	-0.199672859
Vegetative.Length	-0.30987729	0.008542924
Akinetes.Width '	-0.28902837	0.222689552
Glycogen	-0.26433954	0.286827487
u.max.	-0.07919603	-0.621464063
Chlorophyll.a	-0.04857964	-0.616671174

An interesting result from the clustering analysis was that CCM-UFV069 was placed in “sub-cluster-A” branch (Figure 12). This result can be compared with the growth pattern (Figure 8), in which this strain had a more similar aggregation patter with sub-cluster A strains (Figure 6). However, the metabolic parameters put this strain as a distinct organism, as observed in the PCA (Figure 11 and Table 5).

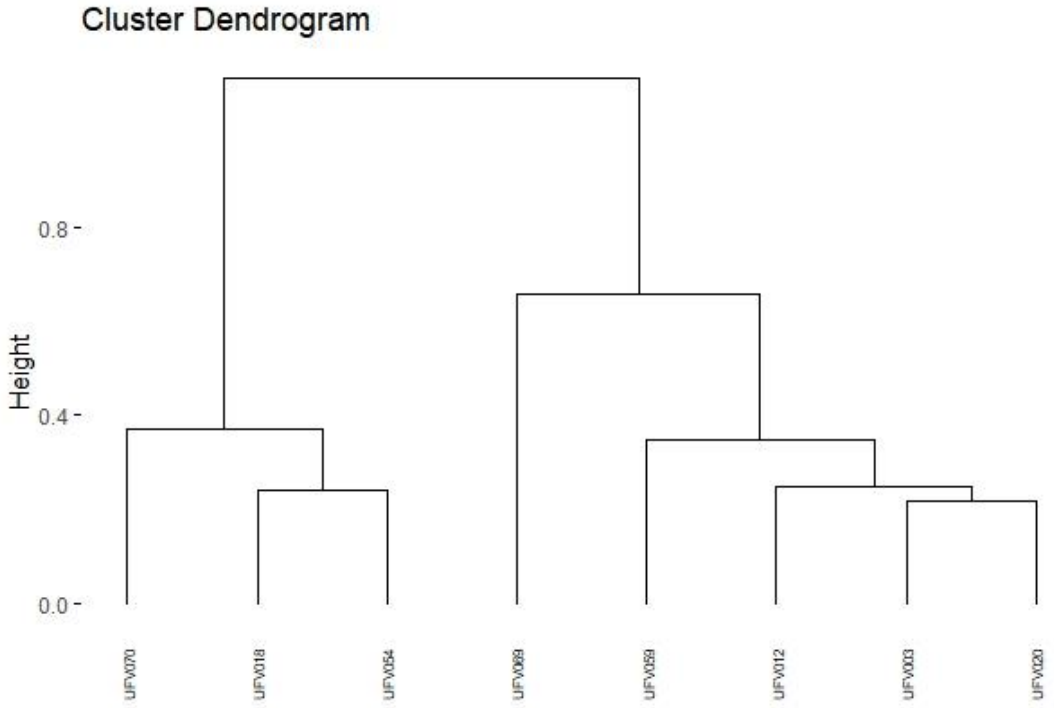

Figure 12. Cluster Dendogram from Ward’s method analysis between the eight *Desmonostoc* strains.

When considered together, the results described here coupled with information available on the literature, shed light on a new perspective for the polyphasic approach, aiming the use of physiological and metabolic data. This corroborate with compelling evidences that highlight that different stable phenotypes of cyanobacteria are not reflected in 16S rRNA gene sequence

comparisons (Mateo et al., 2011). Accordingly, the use of other genetic markers, or the use of distinct characteristics, as physiological and metabolic traits, as pigments quantification, can help to overcome some of the relevant systematics issues.

4. CONCLUSIONS

The results obtained here indicate that *Desmonostoc* genera is seemingly a robust phylogenetic genus, although it harbors a great morphological, metabolic and physiological diversity. Surprisingly, the morphological diversity seems to be relatively greater than previously thought. Our results demonstrated a great diversity on morphological and physiological data inside cluster D1 of *Desmonostoc*. This can be observed by the differences on the strains belonging to sub-cluster A when all data was clustered together in the PCA, further indicating that physiological data are important to solve issues not clearly defined by means of the molecular phylogeny. The photosynthetic parameters indicated that the *Desmonostoc* spp., at least those used here, are “shading” strains. Our sampling site locations shown that *Desmonostoc* spp. are abundant in freshwater environments, yet the majority of *Desmonostoc* spp. described until now were from terrestrial environment.

Interestingly, the lower levels of all measured metabolites observed for CCM-UFV069 facilitate the separation of this strain from the other *Desmonostoc* spp. Notably, CCM-UFV018 and 054 exhibit a different growth pattern and phylogenetic singular position, along with CCM-UFV070. This fact indicates that these strains are most likely novel species and, more importantly, are potential options to biotechnological applications, since they exhibit high protein levels, and homogeneous growth.

Finally, by coupling physiological and metabolic data in a range of *Desmonostoc* strains and further discussing the results of such experiment can give rise to elusive conclusions for the phylogenetical placement of this genera. Thus, the present study raises attention on this often neglected issue and the consequences that it entails within cyanobacterial taxonomy and systematics delimitation of taxa. Collectively, the usage of the approaches here described will likely prove instrumental in defining the hierarchical nature of the cyanobacterial genera that culminated with the potential biotechnological applications of this remarkable organism.

5 REFFERENCES

Alam, S., Brailsford, S.R., Whiley, R.A., Brighton, D., 1999. PCR-based methods for genotyping viridans group streptococci. J. Clin. Microbiol. 37, 2772–2776. https://doi.org/10.1099/00207713-44-4-846

Altschul, S.F., Gish, W., Miller, W., Myers, E.W., Lipman, D.J., 1990. Basic local alignment search tool. J. Mol. Biol. 215, 403–410. https://doi.org/10.1016/S0022-2836(05)80360-2

Anagnostidis, K., 1985. Modern approach to the classification system of cyanophytes 1-Introduction. Arch. Hydrobiol. Suppl. Algol. Stud. 38, 327–472.

Bagchi, S.N., Dubey, N., Singh, P., 2017a. Phylogenetically distant clade of Nostoc-like taxa with the description of *Aliinostoc* gen. Nov. and *Aliinostoc morphoplasticum* sp. nov. Int. J. Syst. Evol. Microbiol. 67, 3329–3338. https://doi.org/10.1099/ijsem.0.002112

Baselga, A., Araújo, M.B., 2010. Do community-level models describe community variation effectively? J. Biogeogr. 37, 1842–1850. https://doi.org/10.1111/j.1365-2699.2010.02341.x

Basheva, D., Moten, D., Stoyanov, P., Belkinova, D., Mladenov, R., Teneva, I., 2018. Content of phycoerythrin, phycocyanin, alophycocyanin and phycoerythrocyanin in some cyanobacterial strains: Applications. Eng. Life Sci. 18, 861–866. https://doi.org/10.1002/elsc.201800035

Berrendero, E., Perona, E., Mateo, P., 2011. Phenotypic variability and phylogenetic relationships of the genera *Tolypothrix* and *Calothrix* (Nostocales, Cyanobacteria) from running water. Int. J. Syst. Evol. Microbiol. 61, 3039–3051. https://doi.org/10.1099/ijs.0.027581-0

Bhunia, A.K., Basu, N.K., Roy, D., Chakrabarti, A., Banerjee, S.K., 1991. Growth, chlorophyll a content, nitrogen-fixing ability, and certain metabolic activities of *Nostoc muscorum*: Effect of methylparathion and benthiocarb. Bull. Environ. Contam. Toxicol. 47, 43–50. https://doi.org/10.1007/BF01689451

Bolhuis, H., Severin, I., Confurius-Guns, V., Wollenzien, U.I.A., Stal, L.J., 2010. Horizontal transfer of the nitrogen fixation gene cluster in the cyanobacterium *Microcoleus chthonoplastes*. ISME J. 4, 121–130. https://doi.org/10.1038/ismej.2009.99

Bornet, E., Flahault, C., 1888. Revision des Nostocacées hétérocystées contenues dans les principaux herbiers de France. Ann. des Sci. Nat. Bot. Septième série 3, 323-381.

Bradford, M.M., 1976. A rapid and sensitive method for the quantitation of microgram quantities of protein utilizing the principle of protein-dye binding. Anal. Biochem. 72, 248–254. https://doi.org/10.1016/0003-2697(76)90527-3

Cadel-Six, S., Dauga, C., Castets, A.M., Rippka, R., Bouchier, C., Tandeau De Marsac, N., Welker, M., 2008. Halogenase genes in nonribosomal peptide synthetase gene clusters of *Microcystis* (Cyanobacteria): Sporadic distribution and evolution. Mol. Biol. Evol. 25, 2031–2041. https://doi.org/10.1093/molbev/msn150

Cai, F., Li, X., Geng, R., Peng, X., Li, R., 2019a. Phylogenetically distant clade of Nostoc-like taxa with the description of *Minunostoc* gen. nov. and *Minunostoc cylindricum* sp. nov. Fottea 19, 13–24.

https://doi.org/10.5507/fot.2018.013
Cai, F., Li, X., Yang, Y., Jia, N., Huo, D., Li, R., 2019b. *Compactonostoc shennongjiaensis* gen. & sp. nov. (Nostocales, Cyanobacteria) from a wet rocky wall in China. Phycologia 58, 200–210. https://doi.org/10.1080/00318884.2018.1541270
Cai, F., Yang, Y., Wen, Q., Li, R., 2018. *Desmonostoc danxiaense* sp. Nov. (Nostocales, Cyanobacteria) from Danxia mountain in China based on polyphasic approach. Phytotaxa 367, 233–244. https://doi.org/10.11646/phytotaxa.367.3.3
Casamatta, D.A., Johansen, J.R., Vis, M.L., Broadwater, S.T., 2005. Molecular and morphological characterization of ten polar and near-polar strains within the oscillatoriales (Cyanobacteria). J. Phycol. 41, 421–438. https://doi.org/10.1111/j.1529-8817.2005.04062.x
Castenholz, R.W., Wilmotte, A., Herdman, M., Rippka, R., Waterbury, J.B., Iteman, I., Hoffmann, L., 2001. Phylum BX. Cyanobacteria, in: Bergey's Manual® of Systematic Bacteriology. Springer New York, New York, NY, pp. 473–599. https://doi.org/10.1007/978-0-387-21609-6_27
Colabella, F., Moline, M., Libkind, D., 2015. UV Sunscreens of Microbial Origin: Mycosporines and Mycosporine- like Aminoacids. Recent Pat. Biotechnol. 8, 179–193. https://doi.org/10.2174/1872208309666150102104520
Corliss, J.O., Bold, H.C., Wynne, M.J., 1979. Introduction to the Algae: Structure and Reproduction, 2. ed. ed, Transactions of the American Microscopical Society. New Jersey: Prentice Hall. https://doi.org/10.2307/3226060
Cross, J.M., Von Korff, M., Altmann, T., Bartzetko, L., Sulpice, R., Gibon, Y., Palacios, N., Stitt, M., 2006. Variation of enzyme activities and metabolite levels in 24 arabidopsis accessions growing in carbon-limited conditions. Plant Physiol. 142, 1574–1588. https://doi.org/10.1104/pp.106.086629
Cuellar-Bermudez, S.P., Aguilar-Hernandez, I., Cardenas-Chavez, D.L., Ornelas-Soto, N., Romero-Ogawa, M.A., Parra-Saldivar, R., 2015. Extraction and purification of high-value metabolites from microalgae: Essential lipids, astaxanthin and phycobiliproteins. Microb. Biotechnol. 8, 190–209. https://doi.org/10.1111/1751-7915.12167
de Alvarenga, L.V., Vieira Vaz, M.G.M., Genuário, D.B., Esteves-Ferreira, A.A., Almeida, A.V.M., de Castro, N.V., Lizieri, C., Souza, J.J.L.L., Schaefer, C.E.G.R., Nunes-Nesi, A., Araújo, W.L., 2018. Extending the ecological distribution of *Desmonostoc* genus: Proposal of *Desmonostoc salinum* sp. nov., a novel Cyanobacteria from a saline–alkaline lake. Int. J. Syst. Evol. Microbiol. 68, 2770–2782. https://doi.org/10.1099/ijsem.0.002878
de Marsac, N.T., Houmard, J., 1988. Complementary chromatic adaptation: Physiological conditions and action spectra, in: Methods in Enzymology. Elsevier, pp. 318–328. https://doi.org/10.1016/0076-6879(88)67037-6
Eduardo, C., Silva, D.F., Gris, B., Sforza, E., La, N., 2016. Effects of Sodium Bicarbonate on Biomass and Carbohydrate Production in *Synechococcus* PCC 7002. Appl. Biochem. Biotechnol. 49, 241–246. https://doi.org/10.3303/CET1649041
Erko, S., Ebers, J., 2006. Taxonomic parameters revisited: tarnished gold

standards, Microbiology Today.
Esteves-Ferreira, A.A., Carvalho, R.A., Vaz, M.G.M. V., Alvarenga, L. V., Barros, K.A., de Castro, N.V., Damatta, F.M., Nunes-Nesi, A., Sulpice, R., Araújo, W.L., 2019. Metabolic and physiological traits in cyanobacterial strains with distinct morphology and ecological origin. J. Phycol. Unpublishe.
Esteves-Ferreira, A.A., Cavalcanti, J.H.F., Vaz, M.G.M.V., Alvarenga, L.V., Nunes-Nesi, A., Araújo, W.L., 2017. Cyanobacterial nitrogenases: Phylogenetic diversity, regulation and functional predictions. Genet. Mol. Biol. 40. https://doi.org/10.1590/1678-4685-gmb-2016-0050
Fergusson, K.M., Saint, C.P., 2000. Molecular phylogeny of Anabaena circinalis and its identification in environmental samples by PCR. Appl. Environ. Microbiol. 66, 4145–4148. https://doi.org/10.1128/AEM.66.9.4145-4148.2000
Fernie, A.R., Roscher, A., Ratcliffe, R.G., Kruger, N.J., 2001. Fructose 2,6-bisphosphate activates pyrophosphate: fructose-6-phosphate 1-phosphotransferase and increases triose phosphate to hexose phosphate cycling in heterotrophic cells. Planta 212, 250–263. https://doi.org/10.1007/s004250000386
Fiore, M.F., Sant'Anna, C.L., Azevedo, M.T.D.P., Komárek, J., Kaštovský, J., Sulek, J., Lorenzi, A.S., 2007. The cyanobacterial genus *Brasilonema*, gen. nov., a molecular and phenotypic evaluation. J. Phycol. 43, 789–798. https://doi.org/10.1111/j.1529-8817.2007.00376.x
Flores, E., Herrero, A., 2010. Compartmentalized function through cell differentiation in filamentous cyanobacteria. Nat. Rev. Microbiol. 8, 39–50. https://doi.org/10.1038/nrmicro2242
Genuário, D.B., Corrêa, D.M., Komárek, J., Fiore, M.F., 2013. Characterization of freshwater benthic biofilm-forming *Hydrocoryne* (Cyanobacteria) isolates from Antarctica. J. Phycol. 49, 1142–1153. https://doi.org/10.1111/jpy.12124
Genuário, D.B., Vaz, M.G.M.V., Melo, I.S. de, 2017. Phylogenetic insights into the diversity of homocytous cyanobacteria from Amazonian rivers. Mol. Phylogenet. Evol. 116, 120–135. https://doi.org/10.1016/j.ympev.2017.08.010
Genuário, D.B., Vieira Vaz, M.G.M., Hentschke, G.S., Sant ' Anna, C.L., Fiore, M.F., 2015. *Halotia* gen. Nov., a phylogenetically and physiologically coherent cyanobacterial genus isolated from marine coastal environments. Int. J. Syst. Evol. Microbiol. 65, 633–675. https://doi.org/10.1099/ijs.0.070078-0
Gugger, M.F., Hoffmann, L., 2004. Polyphyly of true branching cyanobacteria (Stigonematales). Int. J. Syst. Evol. Microbiol. 54, 349–357. https://doi.org/10.1099/ijs.0.02744-0
Gupta, A., Mohan, D., Saxena, R.K., Singh, S., 2018. Phototrophic cultivation of NaCl-tolerant mutant of Spirulina platensis for enhanced C-phycocyanin production under optimized culture conditions and its dynamic modeling. J. Phycol. 54, 44–55. https://doi.org/10.1111/jpy.12597
Henson, B.J., Hesselbrock, S.M., Watson, L.E., Barnum, B.R., 2004. Molecular phylogeny of the heterocystous cyanobacteria (subsections IV and V) based on nifD. Int. J. Syst. Evol. Microbiol. 54, 493–497.

https://doi.org/10.1099/ijs.0.02821-0
Hentschke, G.S., Johansen, J.R., Pietrasiak, N., Rigonato, J., Fiore, M.F., Sant'Anna, C.L., 2017. *Komarekiella atlantica* gen. Et sp. nov. (nostocaceae, cyanobacteria): A new subaerial taxon from the Atlantic rainforest and Kauai, Hawaii. Fottea 17, 178–190. https://doi.org/10.5507/fot.2017.002
Herrero, A., Flores, E., 2019. Genetic responses to carbon and nitrogen availability in *Anabaena.* Environ. Microbiol. 21, 1–17. https://doi.org/10.1111/1462-2920.14370
Hildebrandt, T.M., Nunes Nesi, A., Araújo, W.L., Braun, H.P., 2015. Amino Acid Catabolism in Plants. Mol. Plant 8, 1563–1579. https://doi.org/10.1016/j.molp.2015.09.005
Hoff-Risseti, C., Dörr, F.A., Schaker, P.D.C., Pinto, E., Werner, V.R., Fiore, M.F., 2013. Cylindrospermopsin and Saxitoxin Synthetase Genes in *Cylindrospermopsis raciborskii* Strains from Brazilian Freshwater. PLoS One 8, 35–39. https://doi.org/10.1371/journal.pone.0074238
Hoffmann, L., Komárek, J., Kaštovský, J., 2005. System of cyanoprokaryotes (cyanobacteria) – state in 2004. Arch. Hydrobiol. Suppl. Algol. Stud. 117, 95–115. https://doi.org/10.1127/1864-1318/2005/0117-0095
Hrouzek, P., Lukešová, A., Mareš, J., Ventura, S., 2013. Description of the cyanobacterial genus *Desmonostoc* gen. nov. including *D. muscorum* comb. nov. as a distinct, phylogenetically coherent taxon related to the genus Nostoc. Fottea 13, 201–213. https://doi.org/10.5507/fot.2013.016
Hrouzek, P., Ventura, S., Lukešová, A., Mugnai, M.A., Turicchia, S., Komárek, J., 2009. Diversity of soil *Nostoc* strains: phylogenetic and phenotypic variability. Arch. Hydrobiol. Suppl. Algol. Stud. 117, 251–264. https://doi.org/10.1127/1864-1318/2005/0117-0251
Hrouzek, P., Ventura, S., Lukešová, A., Mugnai, M.A., Turicchia, S., Komárek, J., 2005. Diversity of soil *Nostoc* strains: phylogenetic and phenotypic variability. Arch. Hydrobiol. Suppl. Algol. Stud. 117, 251–264. https://doi.org/10.1127/1864-1318/2005/0117-0251
Jaiswal, A., Koli, D.K., Kumar, A., Kumar, S., Sagar, S., 2018. Pigments analysis of cyanobacterial strains. ~ 1248 ~ Int. J. Chem. Stud. 6, 1248–1251.
Jeon, Y.C., Cho, C.W., Yun, Y.S., 2006. Oxygen evolution rate of photosynthetic microalga *Haematococcus pluvialis* depending on light intensity and quality. Stud. Surf. Sci. Catal. 159, 157–160. https://doi.org/10.1016/s0167-2991(06)81557-0
Katoch, M., Mazmouz, R., Chau, R., Pearson, L.A., Pickford, R., Neilan, B.A., 2016. Heterologous production of cyanobacterial mycosporine-like amino acids mycosporine-ornithine and mycosporine-lysine in *Escherichia coli.* Appl. Environ. Microbiol. 82, 6167–6173. https://doi.org/10.1128/AEM.01632-16
Kaushal, S., Singh, Y., Khattar, J.I.S., Singh, D.P., 2017. Phycobiliprotein production by a novel cold desert cyanobacterium *Nodularia sphaerocarpa* PUPCCC 420.1. J. Appl. Phycol. 29, 1819–1827. https://doi.org/10.1007/s10811-017-1093-7
Khazi, M.I., Demirel, Z., Dalay, M.C., 2018. Evaluation of growth and phycobiliprotein composition of cyanobacteria isolates cultivated in different nitrogen sources. J. Appl. Phycol. 30, 1513–1523.

https://doi.org/10.1007/s10811-018-1398-1
Knoop, H., Gründel, M., Zilliges, Y., Lehmann, R., Hoffmann, S., Lockau, W., Steuer, R., 2013. Flux Balance Analysis of Cyanobacterial Metabolism: The Metabolic Network of *Synechocystis* sp. PCC 6803. PLoS Comput. Biol. 9, e1003081. https://doi.org/10.1371/journal.pcbi.1003081
Komarek, J., 2006. Cyanobacterial Taxonomy: Current Problems and Prospects for the Integration of Traditional and Molecular Approaches. Algae 21, 349–375. https://doi.org/10.4490/algae.2006.21.4.349
Komárek, J., 2010a. Modern taxonomic revision of planktic nostocacean cyanobacteria: A short review of genera. Hydrobiologia 639, 231–243. https://doi.org/10.1007/s10750-009-0030-4
Komárek, J., 2010b. Recent changes (2008) in cyanobacteria taxonomy based on a combination of molecular background with phenotype and ecological consequences (genus and species concept). Hydrobiologia 639, 245–259. https://doi.org/10.1007/s10750-009-0031-3
Komárek, J., Anagnostidis, K., 1989. Modern approach to the classifcation system of cyano-bacteria 4. Nostocales. Arch Hydrobiol Algol Stud 56, 247–345.
Komárek, J., Kaštovský, J., 2003. Coincidences of structural and molecular characters in evolutionary lines of cyanobacteria. Arch. Hydrobiol. Suppl. Algol. Stud. 109, 305–325. https://doi.org/10.1127/1864-1318/2003/0109-0305
Komárek, J., Kaštovský, J., Mareš, J., Johansen, J.R., 2014. Taxonomic classification of cyanoprokaryotes (cyanobacterial genera) 2014, using a polyphasic approach. Preslia 86, 295–335.
Korelusova, J., Kastovsky, J., Komarek, J., 2009. Heterogeneity of the cyanobacterial genus synechocystis and description of a new genus, geminocystis. J. Phycol. 45, 928–937. https://doi.org/10.1111/j.1529-8817.2009.00701.x
Kumar, M., Kulshreshtha, J., Singh, G.P., 2011. Growth and biopigment accumulation of cyanobacterium *Spirulina platensis* at different light intensities and temperature. Brazilian J. Microbiol. 42, 1128–1135. https://doi.org/10.1590/S1517-83822011000300034
Lyra, C., Suomalainen, S., Gugger, M., Vezie, C., Sundman, P., Paulin, L., Sivonen, K., 2001. Molecular characterization of planktic cyanobacteria of *Anabaena, Aphanizomenon, Microcystis* and *Planktothrix* genera. Int. J. Syst. Evol. Microbiol. 51, 513–526. https://doi.org/10.1099/00207713-51-2-513
Mai, T., Johansen, J.R., Pietrasiak, N., Bohunická, M., Martin, M.P., 2018. Revision of the Synechococcales (Cyanobacteria) through recognition of four families including Oculatellaceae fam. nov. and Trichocoleaceae fam. nov. and six new genera containing 14 species. Phytotaxa 365, 1–59. https://doi.org/10.11646/phytotaxa.365.1.1
Mangan, N.M., Flamholz, A., Hood, R.D., Milo, R., Savage, D.F., 2016. PH determines the energetic efficiency of the cyanobacterial CO2 concentrating mechanism. Proc. Natl. Acad. Sci. U. S. A. 113, E5354–E5362. https://doi.org/10.1073/pnas.1525145113
Manoj Kumar, Jyoti Kulshreshtha, G.P.S., 2011. Growth and biopigment accumulation of cyanobacterium. Brazilian J. Microbiol. 42, 1128–1135.
Marsac, N.T., 1994. Differentiation of Hormogonia and Relationships with

Other Biological Processes, in: The Molecular Biology of Cyanobacteria. pp. 825–842. https://doi.org/10.1007/978-94-011-0227-8_28
Mashayekhi, M., Sarrafzadeh, M.H., Tavakoli, O., Soltani, N., Faramarzi, M.A., 2017. Potential for biodiesel production and carbon capturing from *Synechococcus elongatus*: An isolation and evaluation study. Biocatal. Agric. Biotechnol. 9, 230–235. https://doi.org/10.1016/j.bcab.2017.01.005
Mateo, P., Perona, E., Berrendero, E., Leganés, F., Martín, M., Golubić, S., 2011. Life cycle as a stable trait in the evaluation of diversity of *Nostoc* from biofilms in rivers. FEMS Microbiol. Ecol. 76, 185–198. https://doi.org/10.1111/j.1574-6941.2010.01040.x
Miscoe, L.H., Johansen, J.R., Kociolek, J.P., Lowe, R.L., Vaccarino, M.A., Pietrasiak, N., Sherwood, A.R., 2016. Novel cyanobacteria from caves on Kauai, Hawaii, The diatom flora and cyanobacteria from caves on Kauai, Hauwaii. Schweizerbart Science Publishers, Stuttgart, Germany.
Moore, W.E.C., Stackebrandt, E., Kandler, O., Colwell, R.R., Krichevsky, M.I., Truper, H.G., Murray, R.G.E., Wayne, L.G., Grimont, P.A.D., Brenner, D.J., Starr, M.P., Moore, L.H., 1987. Report of the Ad Hoc Committee on Reconciliation of Approaches to Bacterial Systematics. Int. J. Syst. Evol. Microbiol. 37, 463–464. https://doi.org/10.1099/00207713-37-4-463
Muro-Pastor, M.I., Florencio, F.J., 2003. Regulation of ammonium assimilation in cyanobacteria. Plant Physiol. Biochem. 41, 595–603. https://doi.org/10.1016/S0981-9428(03)00066-4
Neilan, B.A., Jacobs, D., Therese, D.D., Blackall, L.L., Hawkins, P.R., Cox, P.T., Goodman, A.E., 1997. rRNA Sequences and Evolutionary Relationships among Toxic and Nontoxic Cyanobacteria of the Genus *Microcystis*. Int. J. Syst. Bacteriol. 47, 693–697. https://doi.org/10.1099/00207713-47-3-693
Nickell, S.P., Stryker, G.A., Arevalo, C., 1993. Isolation from *Trypanosoma cruzi*-infected mice of CD8+, MHC-restricted cytotoxic T cells that lyse parasite-infected target cells. J. Immunol. 150, 1446–57. https://doi.org/10.1128/AEM.69.9.5157
Obuekwe, I.S., Vaz, M.G.M.V., Genuário, D.B., Castro, N.V., Almeida, A.V.M., Veloso, R.W., Pinto, G.N., Alvarenga, L. V., Mello, J. V., Nunes-Nesi, A., Araújo, W.L., 2019. Arsenic-contaminated sediment from mining areas as source of morphological and phylogenetic distinct cyanobacterial lineages. Algal Res. 42, 101589. https://doi.org/10.1016/j.algal.2019.101589
Olson, J.B., Steppe, T.F., Litaker, R.W., Paerl, H.W., 1998. N2-fixing microbial consortia associated with the ice cover of Lake Bonney, Antarctica. Microb. Ecol. 36, 231–238. https://doi.org/10.1007/s002489900110
Otsuka, S., Suda, S., Li, R., Watanabe, M., Oyaizu, H., Matsumoto, S., Watanabe, M.M., 1999. Phylogenetic relationships between toxic and non-toxic strains of the genus *Microcystis* based on 16S to 23S internal transcribed spacer sequence. FEMS Microbiol. Lett. 172, 15–21. https://doi.org/10.1016/S0378-1097(99)00010-5
Pagels, F., Guedes, A.C., Amaro, H.M., Kijjoa, A., Vasconcelos, V., 2019. Phycobiliproteins from cyanobacteria: Chemistry and biotechnological

applications. Biotechnol. Adv. 37, 422–443. https://doi.org/10.1016/j.biotechadv.2019.02.010
Palinska, K.A., Liesack, W., Rhiel, E., Krumbein, W.E., 1996. Phenotype variability of identical genotypes: The need for a combined approach in cyanobacterial taxonomy demonstrated on Merismopedia-like isolates. Arch. Microbiol. 166, 224–233. https://doi.org/10.1007/s002030050378
Papaefthimiou, D., Hrouzek, P., Mugnai, M.A., Lukesova, A., Turicchia, S., Rasmussen, U., Ventura, S., 2008. Differential patterns of evolution and distribution of the symbiotic behaviour in nostocacean cyanobacteria. Int. J. Syst. Evol. Microbiol. 58, 553–564. https://doi.org/10.1099/ijs.0.65312-0
Porra, R.J., Thompson, W.A., Kriedemann, P.E., 1989. Determination of accurate extinction coefficients and simultaneous equations for assaying chlorophylls a and b extracted with four different solvents: verification of the concentration of chlorophyll standards by atomic absorption spectroscopy. BBA - Bioenerg. 975, 384–394. https://doi.org/10.1016/S0005-2728(89)80347-0
Postgate, J.R., 1982. Biology {Nitrogen} {Fixation}: {Fundamentals}. Philos. Trans. R. Soc. Lond. B. Biol. Sci. 296, 375–385.
Ramos, V., Morais, J., Castelo-Branco, R., Pinheiro, Â., Martins, J., Regueiras, A., Pereira, A.L., Lopes, V.R., Frazão, B., Gomes, D., Moreira, C., Costa, M.S., Brûle, S., Faustino, S., Martins, R., Saker, M., Osswald, J., Leão, P.N., Vasconcelos, V.M., 2018. Cyanobacterial diversity held in microbial biological resource centers as a biotechnological asset: the case study of the newly established LEGE culture collection. J. Appl. Phycol. 30, 1437–1451. https://doi.org/10.1007/s10811-017-1369-y
Rantala, A., Fewer, D.P., Hisbergues, M., Rouhiainen, L., Vaitomaa, J., Borner, T., Sivonen, K., 2004. Phylogenetic evidence for the early evolution of microcystin synthesis. Proc. Natl. Acad. Sci. 101, 568–573. https://doi.org/10.1073/pnas.0304489101
Řeháková, K., Johansen, J.R., Casamatta, D.A., Xuesong, L., Vincent, J., 2007. Morphological and molecular characterization of selected desert soil cyanobacteria: three species new to science including *Mojavia pulchra* gen. et sp. {Nov}. Phycologia 46, 481–502. https://doi.org/10.2216/06-92.1
Rippka, R., 1988. Recognition and Identification of Cyanobacteria, in: Methods in Enzymology. Elsevier, pp. 28–67. https://doi.org/10.1016/0076-6879(88)67005-4
Rippka, R., Deruelles, J., Waterbury, J.B., 1979a. Generic assignments, strain histories and properties of pure cultures of cyanobacteria. J. Gen. Microbiol. 111, 1–61. https://doi.org/10.1099/00221287-111-1-1
Rippka, R., Deruelles, J., Waterbury, J.B., 1979b. Generic assignments, strain histories and properties of pure cultures of cyanobacteria. J. Gen. Microbiol. 111, 1–61. https://doi.org/10.1099/00221287-111-1-1
Rippka, Rosmarie, Deruelles, J., Waterbury, J.B., Herdman, M., Stanier, R.Y., 1979. Generic Assignments, Strain Histories and Properties of Pure Cultures of Cyanobacteria. Microbiology 111, 1–61. https://doi.org/10.1099/00221287-111-1-1
Roeselers, G., Stal, L.J., van Loosdrecht, M.C.M., Muyzer, G., 2007.

Development of a PCR for the detection and identification of cyanobacterial nifD genes. J. Microbiol. Methods 70, 550–556. https://doi.org/10.1016/j.mimet.2007.06.011
Rosales-Loaiza, N., Aiello-Mazzarri, C., Gómez, L., Arredondo, B., Morales, E., 2017. Nutritional quality of biomass from four strains of Nostoc and *Anabaena* grown in batch cultures. Int. Food Res. J. 24, 2212–2219.
Sanz, M., Andreote, A.P.D., Fiore, M.F., Dörr, F.A., Pinto, E., 2015. Structural characterization of new peptide variants produced by cyanobacteria from the Brazilian Atlantic Coastal Forest using liquid chromatography coupled to quadrupole time-of-flight tandem mass spectrometry. Mar. Drugs. https://doi.org/10.3390/md13063892
Saraf, A., Dawda, H.G., Suradkar, A., Behere, I., Kotulkar, M., Shaikh, Z.M., Kumat, A., Batule, P., Mishra, D., Singh, P., 2018. Description of two new species of *Aliinostoc* and one new species of *Desmonostoc* from India based on the Polyphasic Approach and reclassification of *Nostoc punensis* to *Desmonostoc punense* comb. nov. FEMS Microbiol. Lett. 365. https://doi.org/10.1093/femsle/fny272
Schirrmeister, B.E., De Vos, J.M., Antonelli, A., Bagheri, H.C., 2013. Evolution of multicellularity coincided with increased diversification of cyanobacteria and the Great Oxidation Event. Proc. Natl. Acad. Sci. U. S. A. 110, 1791–1796. https://doi.org/10.1073/pnas.1209927110
Sciuto, K., Moro, I., 2015. Cyanobacteria: the bright and dark sides of a charming group. Biodivers. Conserv. 24, 711–738. https://doi.org/10.1007/s10531-015-0898-4
Sekar, S., Chandramohan, M., 2008. Phycobiliproteins as a commodity: Trends in applied research, patents and commercialization. J. Appl. Phycol. 20, 113–136. https://doi.org/10.1007/s10811-007-9188-1
Silva, C.S.P., Genuário, D.B., Vaz, M.G.M.V., Fiore, M.F., 2014. Phylogeny of culturable cyanobacteria from Brazilian mangroves. Syst. Appl. Microbiol. 37, 100–112. https://doi.org/10.1016/j.syapm.2013.12.003
Simeunović, J., Bešlin, K., Svirčev, Z., Kovač, D., Babić, O., 2013. Impact of nitrogen and drought on phycobiliprotein content in terrestrial cyanobacterial strains. J. Appl. Phycol. 25, 597–607. https://doi.org/10.1007/s10811-012-9894-1
Smith, A.J., London, J., Stanier, R.Y., 1967. Biochemical basis of obligate autotrophy in blue-green algae and thiobacilli. J. Bacteriol. 94, 972–983.
Soltani, N., Khavari-Nejad, R.A., Yazdi, M.T., Shokravi, S., Fernández-Valiente, E., 2006. Variation of nitrogenase activity, photosynthesis and pigmentation of the cyanobacterium Fischerella ambigua strain FS18 under different irradiance and pH values. World J. Microbiol. Biotechnol. 22, 571–576. https://doi.org/10.1007/s11274-005-9073-5
Somero, G.N., 1992. Biochemical ecology of deep-sea animals. Experientia 48, 537–543. https://doi.org/10.1007/BF01920236
Spolaore, P., Joannis-cassan, C., Duran, E., 2006. Commercial Applications of Microalgae 101, 87–96. https://doi.org/10.1263/jbb.101.87
Stal, L.J., 2015. Nitrogen Fixation in Cyanobacteria, in: ELS. John Wiley & Sons, Ltd, Chichester, UK, pp. 1–9. https://doi.org/10.1002/9780470015902.a0021159.pub2
Stanier, R.Y., Kunisawa, R., Mandel, M., Cohen-Bazire, G., 1971. Purification and properties of unicellular blue-green algae (order Chroococcales).

Bacteriol. Rev. 35, 171–205.
Stomp, M., Van Dijk, M.A., Van Overzee, H.M.J., Wortel, M.T., Sigon, C.A.M., Egas, M., Hoogveld, H., Gons, H.J., Huisman, J., 2008. The timescale of phenotypic plasticity and its impact on competition in fluctuating environments. Am. Nat. 172, E169–E185. https://doi.org/10.1086/591680
Tamas, I., Svircev, Z., Andersson, S.G.E., 2000. Determinative value of a portion of the nifH sequence for the genera *Nostoc* and *Anabaena* (Cyanobacteria). Curr. Microbiol. 41, 197–200. https://doi.org/10.1007/s00284010118
Taton, A., Grubisic, S., Ertz, D., Hodgson, D.A., Piccardi, R., Biondi, N., Tredici, M.R., Mainini, M., Losi, D., Marinelli, F., Wilmotte, A., 2006. {POLYPHASIC} {STUDY} {OF} {ANTARCTIC} {CYANOBACTERIAL} {STRAINS}. J. Phycol. 42, 1257–1270. https://doi.org/10.1111/j.1529-8817.2006.00278.x
Torzillo, G., Bernardini, P., Masojídek, J., 1998. On-line monitoring of chlorophyll fluorescence to assess the extent of photoinhibition of photosynthesis induced by high oxygen concentration and low temperature and its effect on the productivity of outdoor cultures of *Spirulina platensis* (Cyanobacteria). J. Phycol. 34, 504–510. https://doi.org/10.1046/j.1529-8817.1998.340504.x
Vaz, M.G.M.V., Genuário, D.B., Andreote, A.P.D., Malone, C.F.S., Sant'Anna, C.L., Barbiero, L., Fiore, M.F., 2015. *Pantanalinema* gen. nov. and *Alkalinema* gen. nov.: Novel pseudanabaenacean genera (Cyanobacteria) isolated from saline–alkaline lakes. Int. J. Syst. Evol. Microbiol. 65, 298–308. https://doi.org/10.1099/ijs.0.070110-0
Vitousek, P., Howarth, R., 1991. Nitrogen limitation on land and in the sea: {How} can it occur? Biogeochemistry 13. https://doi.org/10.1007/bf00002772
Walsby, A.E., Hayes, P.K., 1989. Gas vesicle proteins. Biochem. J. 264, 313–322. https://doi.org/10.1042/bj2640313
Whitton, B.A., 2013. Preface. Ecol. Cyanobacteria II Their Divers. Sp. Time 9789400738, v–vi. https://doi.org/10.1007/978-94-007-3855-3
Zehr, J.P., Mellon, M.T., Hiorns, W.D., 1997. Phylogeny of cyanobacterial {nifH} genes: evolutionary implications and potential applications to natural assemblages. Microbiology 143, 1443–1450. https://doi.org/10.1099/00221287-143-4-1443
Zehr, J.P., Turner, P.J., 2001. Nitrogen fixation: Nitrogenase genes and gene expression. Methods Microbiol. 30, 271–286. https://doi.org/10.1016/s0580-9517(01)30049-1
Zhang, C.C., Zhou, C.Z., Burnap, R.L., Peng, L., 2018. Carbon/Nitrogen Metabolic Balance: Lessons from Cyanobacteria. Trends Plant Sci. 23, 1116–1130. https://doi.org/10.1016/j.tplants.2018.09.008